NAVAL POSTGRADUATE SCHOOL
Monterey, California

THESIS

TESTING AND DEVELOPMENT OF A SHROUDED GAS TURBINE ENGINE IN A FREEJET FACILITY

by

Hector Garcia

December 2000

Thesis Advisor: Garth V. Hobson
Thesis Co-Advisor: K.E.Woehler

Approved for public release; distribution is unlimited

REPORT DOCUMENTATION PAGE

Form Approved
OMB No. 0704-0188

1. AGENCY USE ONLY *(Leave blank)*	2. REPORT DATE	3. REPORT TYPE AND DATES COVERED
	December 2000	Master's Thesis

4. TITLE AND SUBTITLE Testing and Development of a Shrouded Gas Turbine Engine in a Freejet Test Facility

5. FUNDING NUMBERS

6. AUTHOR(S)
Hector Garcia

7. PERFORMING ORGANIZATION NAME(S) AND ADDRESS(ES)
Naval Postgraduate School
Monterey, CA 93943-5000

8. PERFORMING ORGANIZATION REPORT NUMBER

1. SPONSORING / MONITORING AGENCY NAME(S) AND ADDRESS(ES)

10. SPONSORING / MONITORING AGENCY REPORT NUMBER

11. SUPPLEMENTARY NOTES
The views expressed in this thesis are those of the author and do not reflect the official policy or position of the Department of Defense or the U.S. Government.

12a. DISTRIBUTION / AVAILABILITY STATEMENT
Approved for public release; distribution is unlimited.

12b. DISTRIBUTION CODE

13.ABSTRACT *(maximum 200 words)*

Testing and analysis of a shrouded turbojet engine with possible application for high speed propulsion on low cost Unmanned Combat Aerial Vehicles (UCAV), Unmanned Aerial Vehicles (UAV) and missiles. The possibility of a turbojet providing thrust at subsonic conditions and the ramjet section providing the thrust in the supersonic regime exists. The combined cycle engine (CCE) could be incorporated into a variety of applications.

The building of a new freejet facility and engine test rig at the Naval Postgraduate School enabled dynamic testing of the ongoing development of a turboramjet.

The freejet facility and new engine stand performed without exception. The shrouded engine was dynamically tested in a freejet up to Mach 0.4. The engine performance measurements closely matched those predicted by a cycle analysis program, GASTURB.

Computational fluid dynamics (CFD) was used to analyze the supersonic inlet at a design point of Mach 2. The results provided by the CFD code, OVERFLOW, matched theoretical flow parameters. The intake design was slightly modified to enhance performance of shock waves in the supersonic flight regime.

14. SUBJECT TERMS	15. NUMBER OF PAGES
Micro-turbojet, GASTURB, Engine shroud, Turboramjet, Sophia J450, Microturbine Performance	92
	16. PRICE CODE

17. SECURITY CLASSIFICATION OF REPORT	18. SECURITY CLASSIFICATION OF THIS PAGE	19. SECURITY CLASSIFI- CATION OF ABSTRACT	20. LIMITATION OF ABSTRACT
Unclassified	Unclassified	Unclassified	UL

NSN 7540-01-280-5500

Standard Form 298 (Rev. 2-89)
Prescribed by ANSI Std.239-18, 298

THIS PAGE IS INTENTIONALLY LEFT BLANK

Approved for public release; distribution is unlimited

TESTING AND DEVELOPMENT OF A SHROUDED GAS TURBINE ENGINE IN A FREEJET FACILITY

Hector Garcia
Lieutenant Commander, United States Navy
B.S., University of California - Riverside, 1986

Submitted in partial fulfillment of the
requirements for the degree of

MASTER OF SCIENCE IN APPLIED PHYSICS

from the

NAVAL POSTGRADUATE SCHOOL
December 2000

Author: 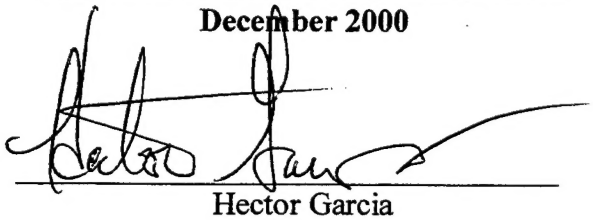
Hector Garcia

Approved by: 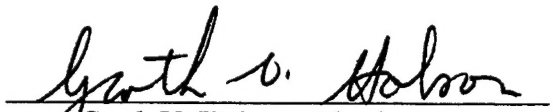
Garth V. Hobson, Thesis Advisor

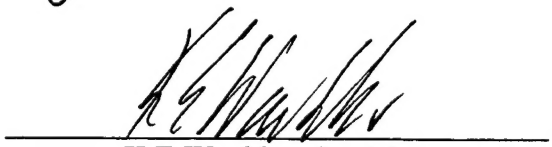
K.E. Woehler, Co-Advisor

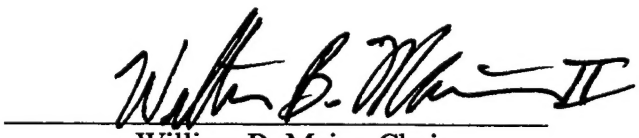
William B. Maier, Chair
Department of Combat System and Physics

THIS PAGE IS INTENTIONALLY LEFT BLANK

ABSTRACT

Testing and analysis of a shrouded turbojet engine with possible application for high speed propulsion on low cost Unmanned Combat Aerial Vehicles (UCAV), Unmanned Aerial Vehicles (UAV) and missiles. The possibility of a turbojet providing thrust at subsonic conditions and the ramjet section providing the thrust in the supersonic regime exists. The combined cycle engine (CCE) could be incorporated into a variety of applications.

The building of a new freejet facility and engine test rig at the Naval Postgraduate School enabled dynamic testing of the ongoing development of a turboramjet.

The freejet facility and new engine stand performed without exception. The shrouded engine was dynamically tested in a freejet up to Mach 0.4. The engine performance measurements closely matched those predicted by a cycle analysis program, GASTURB.

Computational fluid dynamics (CFD) was used to analyze the supersonic inlet at a design point of Mach 2. The results provided by the CFD code, OVERFLOW, matched theoretical flow parameters. The intake design was slightly modified to enhance performance of shock waves in the supersonic flight regime.

THIS PAGE IS INTENTIONALLY LEFT BLANK

TABLE OF CONTENTS

LIST OF FIGURES

LIST OF TABLES

THIS PAGE IS INTENTIONALLY LEFT BLANK

ACKNOWLEDGEMENT

I would like to extend my wholehearted appreciation in acknowledging several people whose efforts greatly contributed towards the completion of this thesis.

Thanks to Mr. Rick Still, Mr. John Gibson and Mr. Doug Seivwright out at the Turbo Propulsion Lab.

I most notably thank my thesis advisor Dr. Garth Hobson of the Department of Aeronautics and Astronautics for giving me the opportunity to work with him in his ambitious research project. His untiring support and guidance enabled the completion of this research.

Most of all I would like to thank my lovely wife, Michelle and all my beautiful children, Bethany, Danae, Casi and Alex. Without their love and support I couldn't have accomplished this undertaking.

I. INTRODUCTION

Missile technology is running on both evolutionary and revolutionary tracks. Evolution will be the path for the near to mid-term, but revolutionary changes in high – speed propulsion could emerge in a decade if tests and development in the next several years prove successful.

The hypersonic transport propulsion system research (HYPR) project was launched in 1989 as a ten-year project. The program is the first large-scale international collaboration research sponsored by Japan's Ministry of International Trade and Industry (MITI). The participants are three Japanese Aero-engine companies (IHI, KHI and MHI), four foreign companies (GE, PWA, RR, and SNECMA) and four Japanese national laboratories (NAL MEL, NRLM and ONRI). The purpose of this project was to develop technologies for a Mach 5 propulsion system for a high speed transport (HST) airplane of the early 21 century, which could be environmentally acceptable and economically viable. The combined cycle engine, composed of a variable cycle engine (VCE) and a ramjet engine, was being studied. A combined cycle engine demonstrator (HYPR90-C) was designed, manufactured and the first sea-level engine tests have been carried out successfully in February 1998. The (HYPR90-C) altitude tests were carried out at the altitude test facility at GE in early spring of 1999. The Combined Cycle Engine (CCE) was successfully tested with the turbojet to ramjet transition mode of operation. It is believed that the CCE in the HYPR project was the first turboramjet engine for commercial use in the world.

Northrup Grumman has turned to tailoring modifications of existing unmanned air vehicle to capture new markets. There was a study with the Defense Advanced Research Projects Agency (DARPA) to transform the Miniature Air Launched Decoys (MALD) into low cost cruise missile interceptors. The Miniature Air Launched Interceptor (MALI) would use a small turbojet engine to propel the vehicle to Mach 1.3. The MALI concept was also planned for adaptation to the Army's Patriot Batteries for ground-launched cruise missile interceptors.

As NATO and the United States continue to expand the use of UAVs, different types of propulsion systems are being studied. Many programs are aimed at cutting the size of current propulsion systems. DARPA has kicked off the Small Scale Propulsion Systems program to enable the development of a new class of aerospace vehicles. The propulsion technology would be used on vehicles ranging in size from 6 inches (Micro Air Vehicles) to 90 inches (Miniature Air Launched Decoy).

In the last few years, the Turbo Propulsion Laboratory (TPL) of the Naval Postgraduate School (NPS) has been studying low-cost, combined-cycle engines for possible high-speed unmanned aerial vehicle (UAV) and missile applications. In 1998, Rivera (Ref. 1), began testing the compressor performance of a Garrett T1.5 turbocharger. This turbocharger was similar to the rotor used in the Sophia J450 engine which is a low-cost turbojet for model aircraft. He also bench tested the Sophia J450, and compared the results to the previously documented tests conducted on another small turbojet engine tested by Lobik (Ref. 2), the JPX-240. Rivera also investigated the on- and off-design performance of the Sophia J450 turbojet engine using a cycle analysis

program GASTURB (Ref. 3), incorporating the experimentally determined Garrett T1.5 compressor map. The performance predictions were favorably compared to off-design tests of the Sophia J450.

In March 1999, Hackaday (Ref. 4) performed a study of the static performance of the Sophia J450 with a constant area ejector. The compressor map for the actual rotor within the J450 was obtained and used with GASTURB to better predict the off-design performance. An engine shroud was manufactured and measurements were made as an initial setup in the consideration of a combined cycle engine.

In September 1999, Andreou (Ref. 5), tested the Sophia J450 inside a shroud of varying configurations, to compare the performance of different duct lengths. Pressure measurements were also performed along the length of the various duct configurations to determine the amount of secondary flow entrainment into the shroud. An elliptical engine intake was designed and tested with two of the shroud configurations.

In June 2000, Namani (Ref. 6) continued the development of a ducted turbojet engine. The static performance was repeated and verified under prolonged testing at different engine speeds. The prolonged running of the engine was determined with an instrumented version of the Sophia J450 capable of being remotely controlled. This version of the engine (denoted J450-2) allowed the accurate measurement of engine shaft rotational speed and exhaust gas temperature through a ground support unit (GSU) and engine control unit (ECU). The continuous engine runs allowed efficient evaluation of the performance and shroud pressures of the uninstrumented engine (J450-1). The design of a supersonic intake was initiated and completed.

In the present thesis a new freejet facility and engine test stand was constructed, so that forward flight conditions could be simulated whilst testing the combined cycle engine. The designed supersonic intake was manufactured and used in conjunction with the medium engine shroud which provided the best performance (Ref. 6). The engine performance was tested within the new test stand. The freejet enabled the performance testing of the shrouded J450 with the supersonic intake in a subsonic air stream at sea level. A computational fluid dynamics study was initiated to explore the external compression of the supersonic intake at the design free stream Mach number of 2.0 because the dynamic testing of the engine was only up to a Mach number of 0.4.

II. ENGINE TEST PROGRAMS

A. EXPERIMENTAL SETUP

1. Overview

The Sophia J450 is the smallest commercially available turbojet engine. Although small in size, the J450 design and principle of operation is very much the same as a full-scale jet engine. The J450 used heavy fuel which was a kerosene/Coleman lantern fuel mixture. Pertinent performance specifications are listed below as Table 1.

SOPHIA J450 ENGINE SPECIFICATION	
Length / Diameter	13.19 / 4.72 [in]
Total weight	4 [lb]
Fuel	Coleman/Kerosene
Starting System	Compressed air
Ignition system	Glow plug
Lubrication	6V pulsed oil pump
Fuel feed system	12V turbine fuel pump
Compressor	Single stage centrifugal
Thrust	11[lbf] at 123000 [RPM]
Fuel consumption	19.98 [lbm/hr]
Throttle system	Remote control/Manual control

Table 1. Sophia J450 Specifications After Refs [1] and [2]

2. Engine Test Rig

The new engine test rig used for the shrouded Sophia J450 is located in the Gas Dynamics Laboratory (Building 216) at the Naval Postgraduate School. It is similar to the same apparatus that was designed by Lobik on 1995 (Ref. 2) for the JPX-240 test program with several minor modifications such as the engine control unit (ECU) which consisted of a fuel pump, oil pump and remote control transmitter. Schematics of the test rig components are shown below in Figure 1.

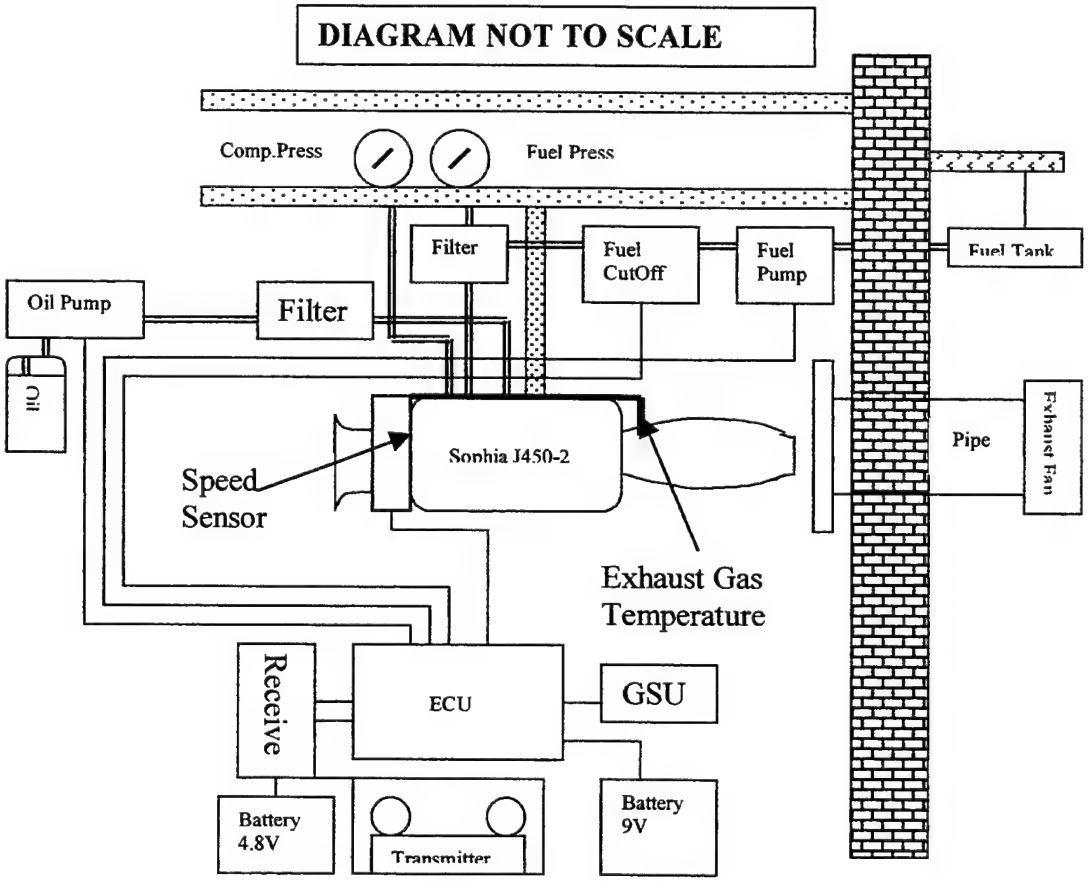

Figure 1. Engine Test Rig

3. Freejet

The newly designed freejet facility was constructed in alignment with the newly constructed engine thrust stand. The freejet can provide up to transonic airflow. The airflow can be provided by a continuous air compressor or from large air storage tanks. The 4 inch exhaust nozzle for the freejet was used for the dynamic testing. The thrust stand was constructed of a 2" x ½" aluminum beam which was strain-gaged. The thrust beam was also enclosed in an elliptic tube to minimize aerodynamic drag from the freejet flow. The thrust beam could freely flex within the elliptical tube.

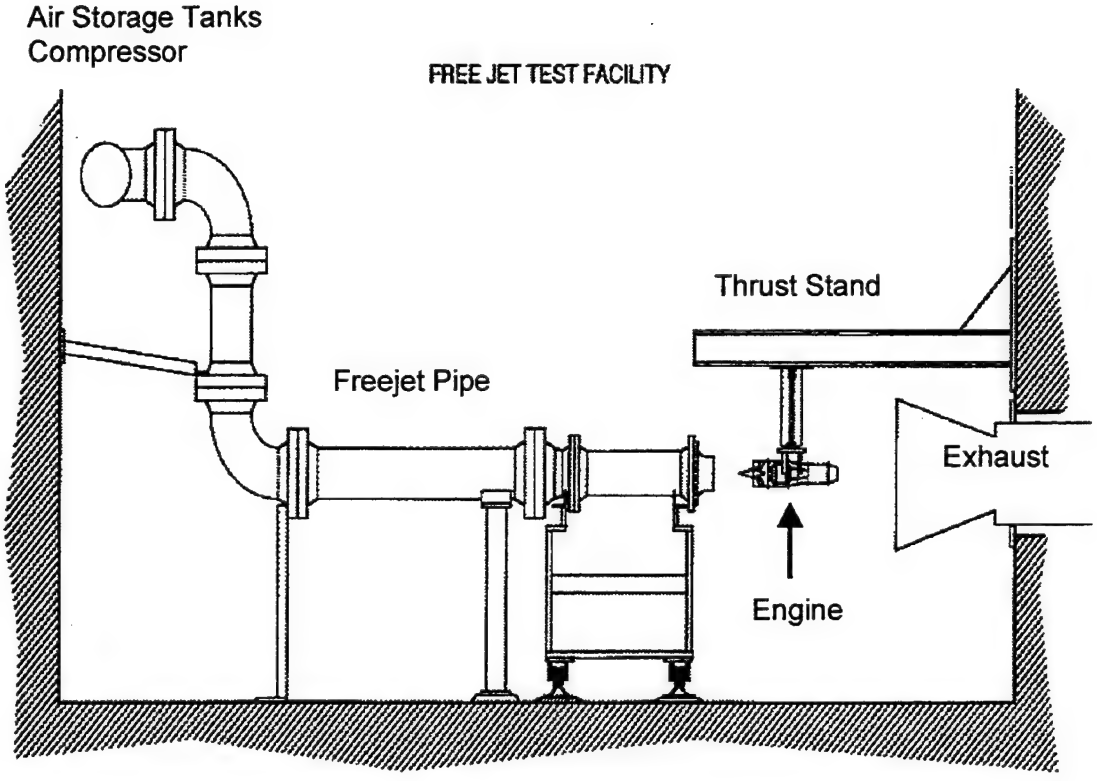

Figure 2. Freejet Facility

B. DATA ACQUISITION AND REDUCTION

1. Overview

A schematic of the Data Acquisition Control Unit [DACU] is shown in Figure 3. The HP9000 Series 300 workstation was used to control the data acquisition system and to store the process the data. The primary instruments used for data acquisition where strain gages. The strain readings were obtained using a [HP6944A] DACU in conjunction with a HP digital voltmeter [DVM], which received signals through a signal conditioner. The DACU, DVM, and multi-programmer were connected to the workstation via a [HP6944A [IEEE-488] bus.

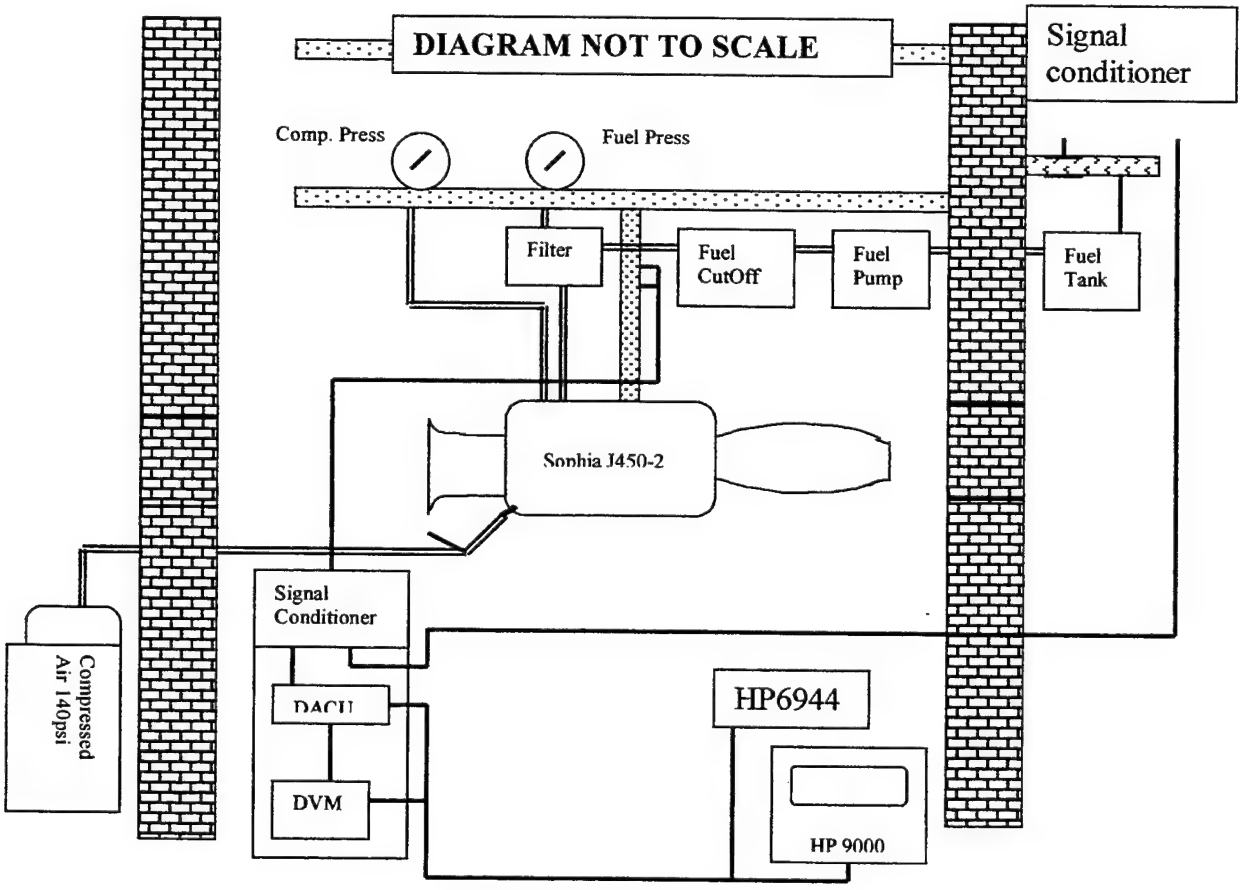

Figure 3. Data Acquisition

2. Instrumentation and Control

a. Thrust Measurements

The engine thrust was determined by using the beam from which the engine was suspended as a thrust-measuring device. The arrangement is shown in Figure 4. The beam contained four strain-gages [two on each side], which were configured in a full Whetstone bridge with the leads providing an output through a signal conditioner to the data acquisition system. The Digital Voltmeter was used to zero out the bridge prior to performing the calibration through channel six on the front panel of the signal conditioner panel. Prior to engine testing, the beam was calibrated both positive and negative, with different weights hung off the engine within the range of engine thrust and drag, as shown below in Figure 4. The calibration results are provided in Appendix B as Table 7.

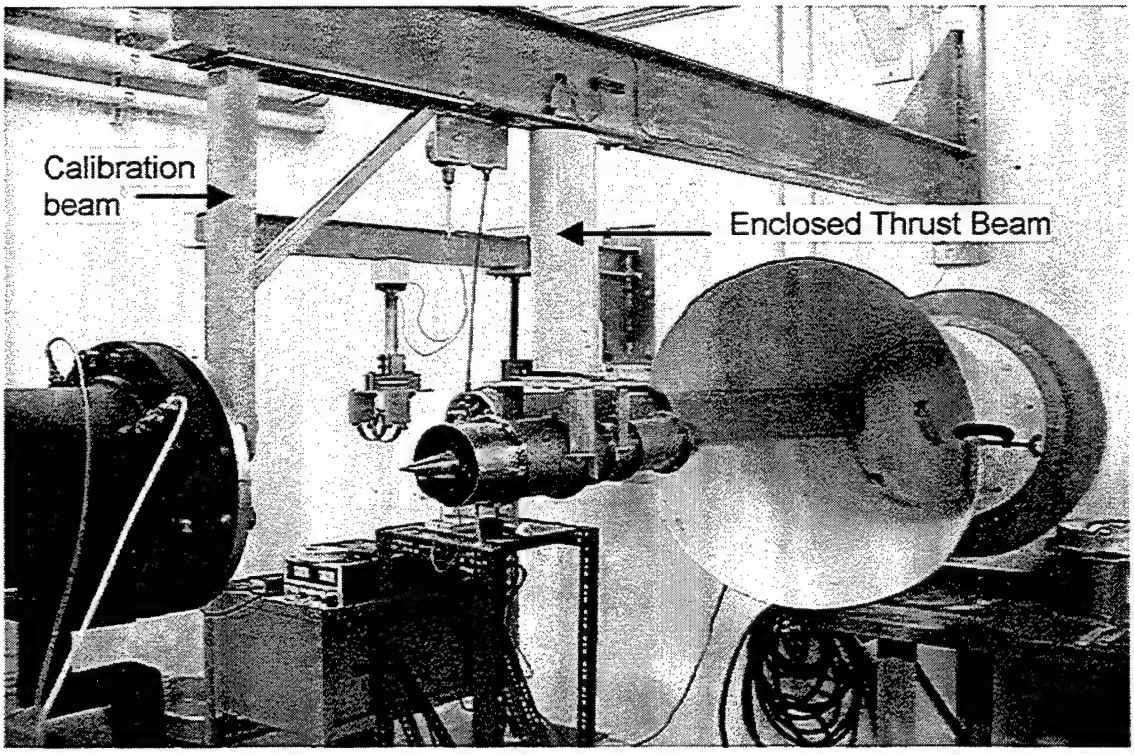

Figure 4. Photograph of the Thrust Measurement System and its Calibration Arrangement

b. Fuel Flow Rate Measurements

The fuel flow rate was determined by using a newly constructed cantilevered beam as a weighing device to calculate the change in fuel weight over given periods of time. The arrangement is shown in Figure 5. The beam used two strain-gages configured in a half Whetstone bridge to provide an output through a signal conditioner to the data acquisition system. Prior to engine testing, the beam was calibrated with known different weights. The calibration results are provided in Appendix B as Table 6.

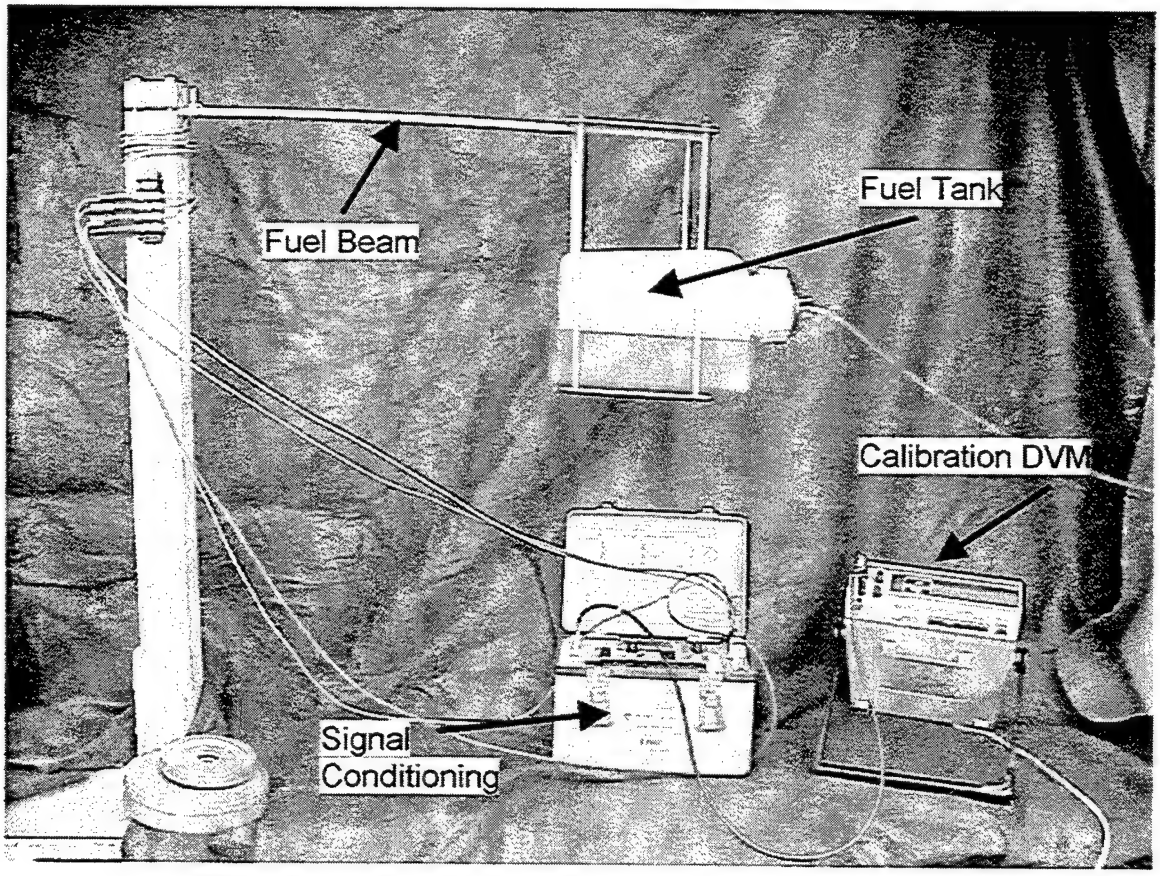

Figure 5. Photograph of the Fuel Weight Measurement

c. Freejet Measurements

The flow rate out of the freejet was determined by measuring the pressure in the duct located upstream of the convergent nozzle. The gage arrangement is shown in Figure 6.

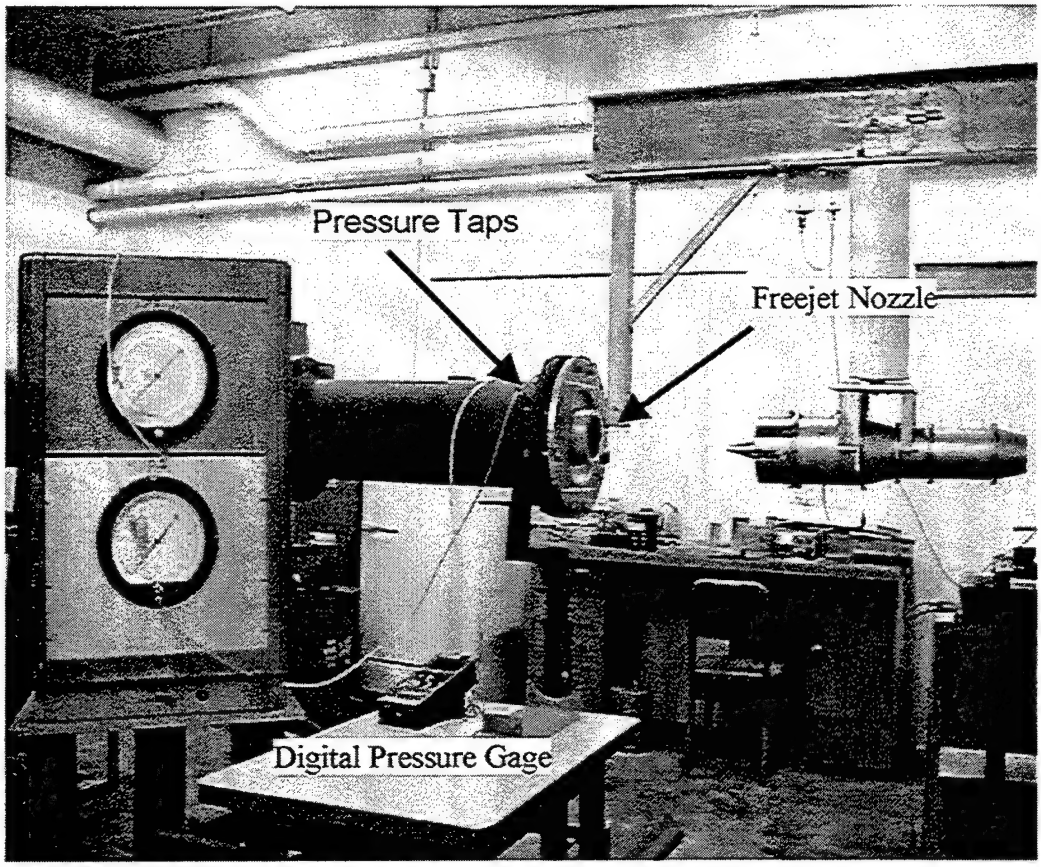

Figure 6. Photograph of the Pressure Measurement of the Freejet

C. RESULTS OF SOPHIA SHROUDED ENGINE TEST PROGRAM

1. Engine Tests with the Intake Removed

Four performance measurements were conducted on the medium shrouded engine with its intake removed at 105%, 100%, 90% and 80% spool speed, respectively at each speed, thrust and fuel flow rate were recorded, the results of which are provided in Appendix C. Figure 7 is of Thrust vs spool speed and Figure 8 is Specific Fuel Consumption (SFC) vs spool speed. The results are averaged and summarized in Table 2.

RUN	Thrust (lbs.)	SFC (lbm/lb./hr)	Spool Speed (RPM)[%]
1	9.9304	1.7239	125000 [105%]
2	8.5775	1.7581	120000 [100%]
3	6.8328	1.8399	109000 [90%]
4	4.4952	2.1689	93000 [80%]
5	1.8455	3.6196	62000 [IDLE]

Table 2. Engine Test Program - No Intake

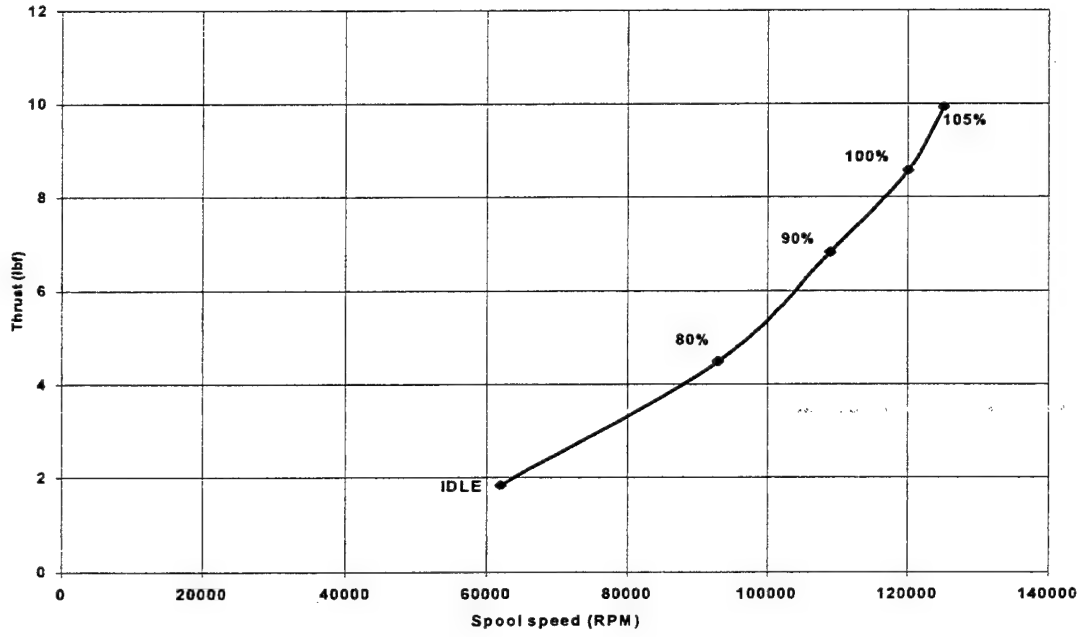

Figure 7. Thrust vs. Spool Speed

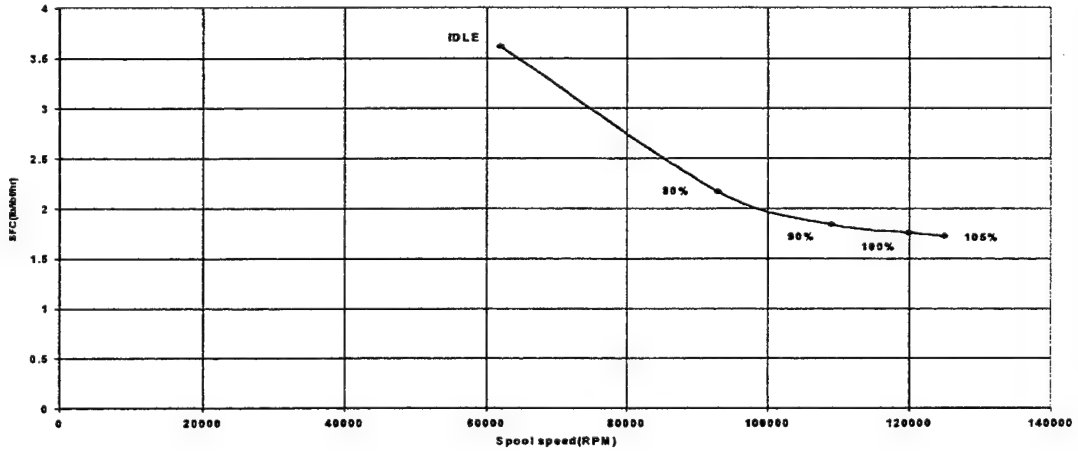

Figure 8. SFC vs. Spool Speed

2. Engine with Conical Intake

The same four engine speeds were conducted on the engine with the supersonic intake. For each run data were recorded for SFC, spool speed and Thrust which are provided in Appendix C. Figures 9 and 10 are of Thrust vs. spool speed and SFC vs. spool speed. Thrust respectively, the results are averaged and summarized in Table 3 as below. A schematic of the engine in the shroud is shown in Figure 11. A photograph of medium shroud with conical intake installation in the stand is shown in Figure 12.

RUN	Thrust(lbs.)	SFC(lbm/lb./hr)	Spool Speed (RPM)[%]
1	9.4525	1.8055	125000 [105%]
2	8.1775	1.8260	120000 [100%]
3	6.534	1.9338	109000 [90%]
4	4.1753	2.3281	93000 [80%]
5	1.6077	4.2990	62000 [IDLE]

Table 3. Engine Test Program Conical Intake

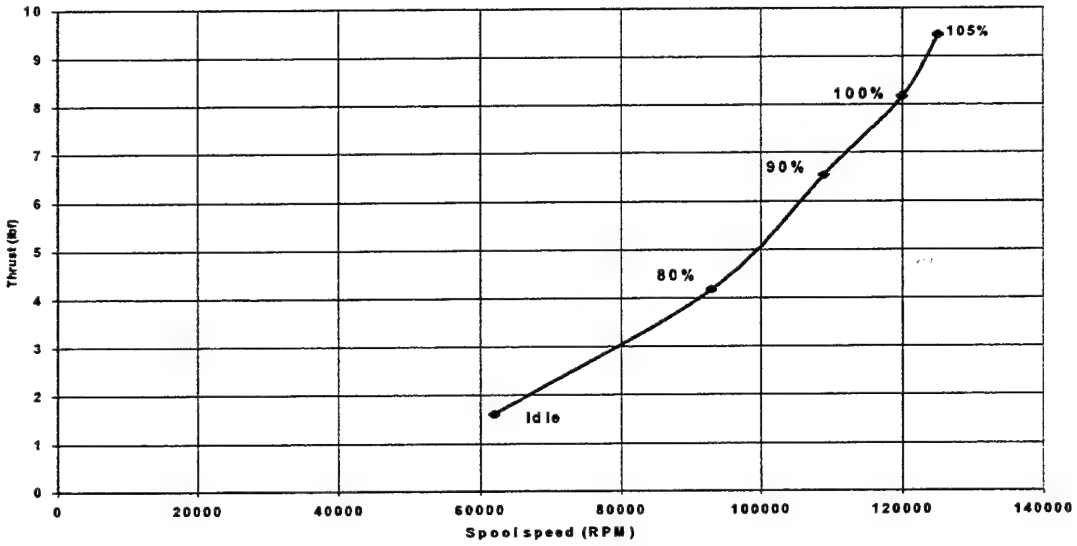

Figure 9. Thrust vs. Spool Speed

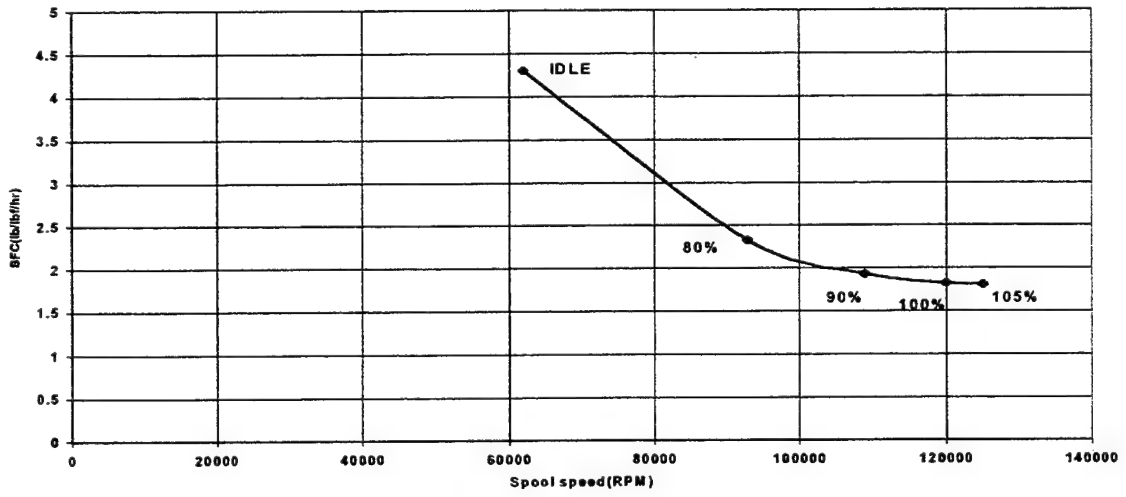

Figure 10. SFC vs. Spool Speed

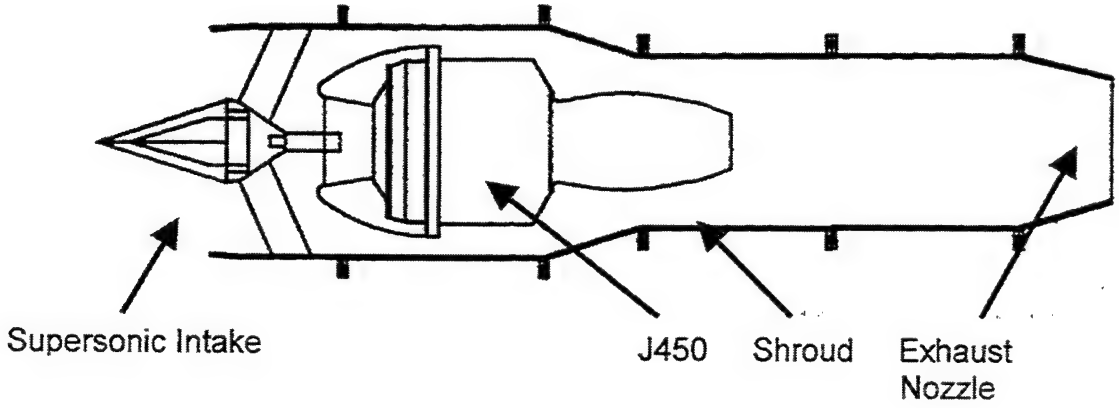

Figure 11. Shrouded J450

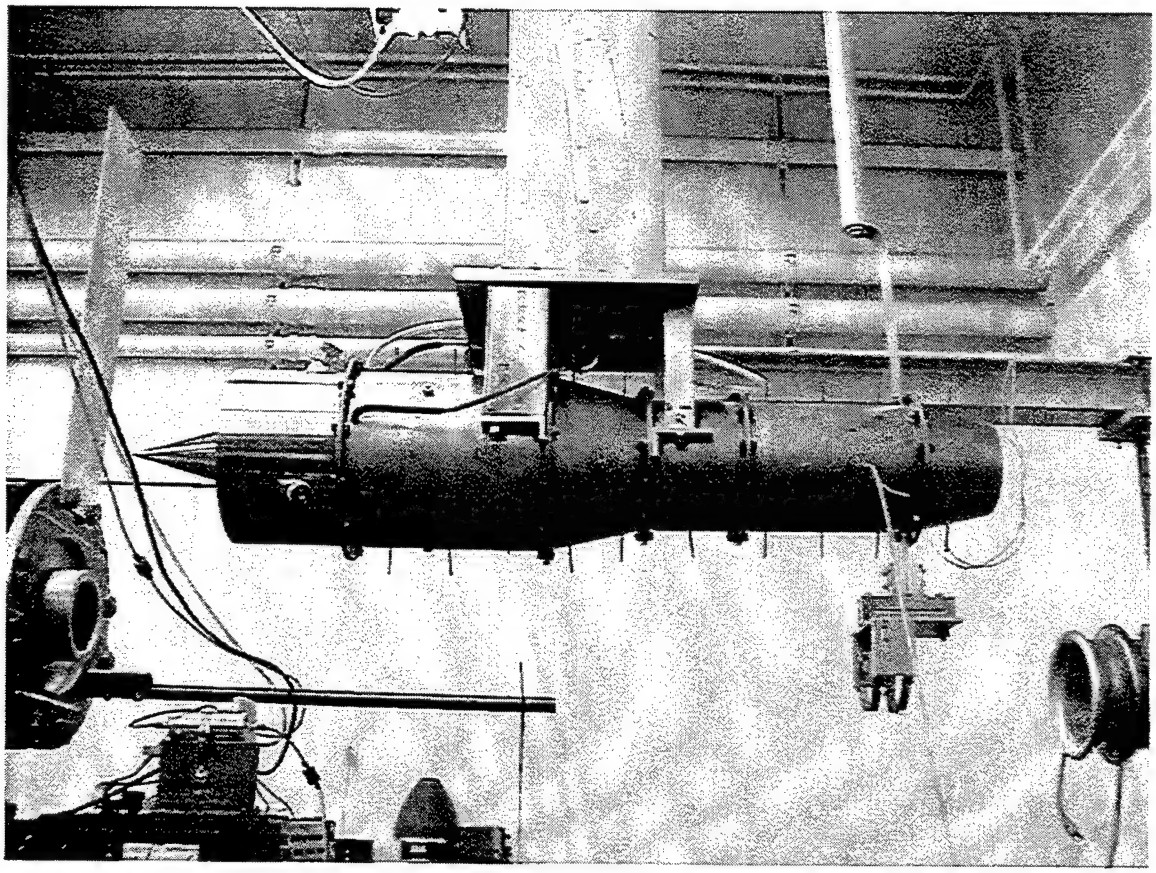

Figure 12. Photograph of the Shrouded Engine

D. SUMMARY AND COMPARSION OF RESULTS

1. Comparison of Different Intakes with Baseline Intake

Figure 13 shows the comparison, at 105%, 100%, 90%, 80% and Idle spool speed, of the different intakes on the Shrouded J450. The conical and elliptical intake (Ref. 6) performances are essentially the same throughout the performance envelope. The conical and elliptical intakes produce approximately 4% less thrust across the performance envelope.

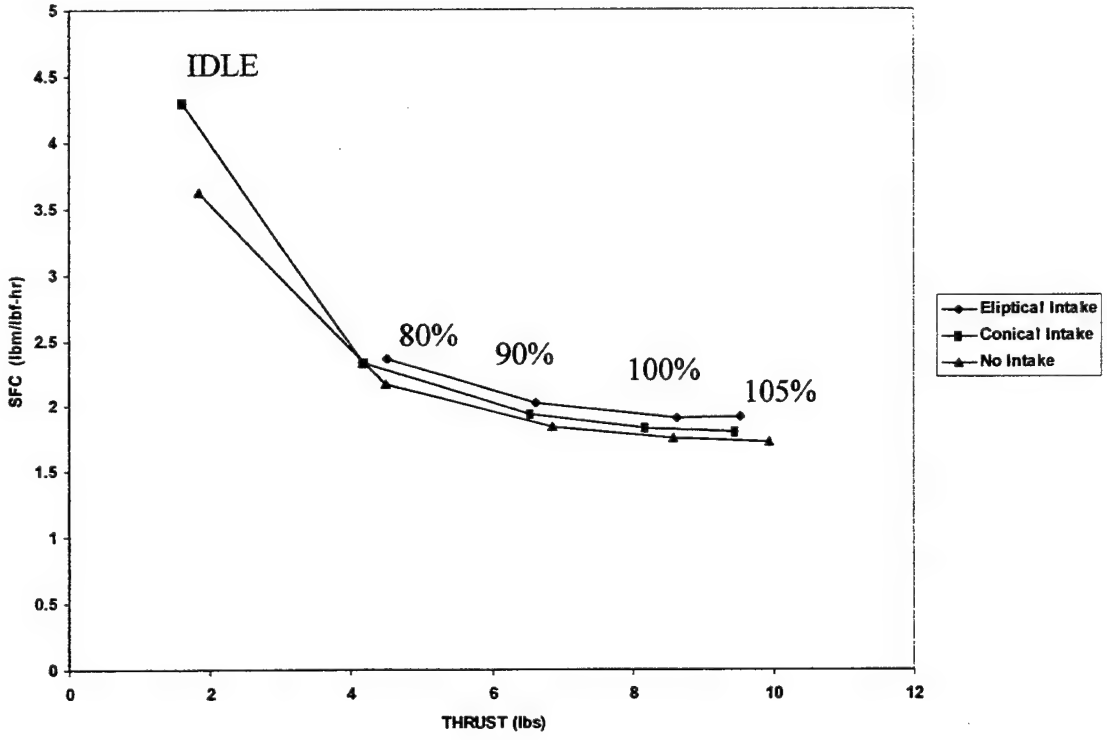

Figure 13. Performance Comparison with Different Intake Configurations

E. FREEJET RESULTS ON SHROUDED ENGINE

1. Freejet Operating on Non-Running Shrouded Engine

The freejet was run with air supplied by the large storage tanks. The starting value of pressure was around 2.0 PSIG ahead of the freejet exhaust nozzle. The starting pressure was obtained by manually bumping open the valve to achieve the desired flow rate. As the air tanks were depleted pressure measurements were taking along with the force (or drag) measurements which are provided in Appendix C, Table 11A. Figure 14 is the Force (or drag) on the engine vs. Mach number.

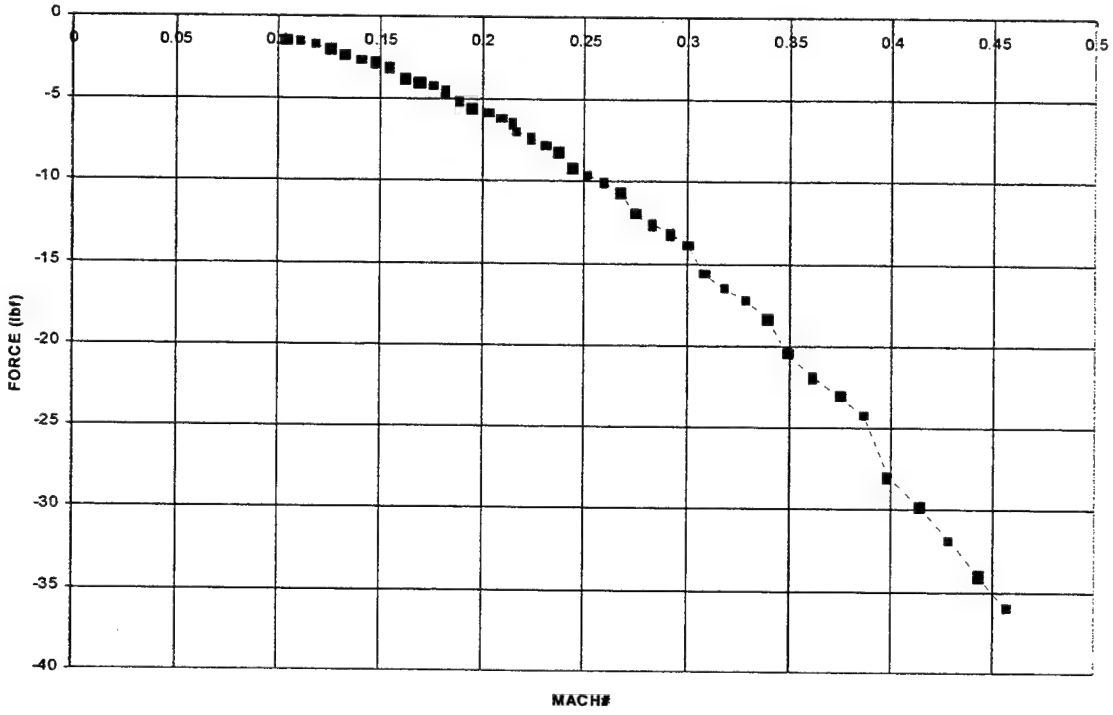

Figure 14. Subsonic Drag Characteristic of the Engine

2. The Shrouded Engine at 100% Spool Speed in the Freejet Flow

The Freejet was run with air supplied by the large storage tanks. The starting value of pressure required was once again around 2.0 PSIG through the freejet exhaust nozzle. The engine was started and run up to 100% operating RPM while the starting air pressure value was achieved. As the air storage tanks were depleted, pressure and force measurements were collected which are provided in Appendix C, Table 11B. Figure 15 is the Force vs. Mach number for this test case.

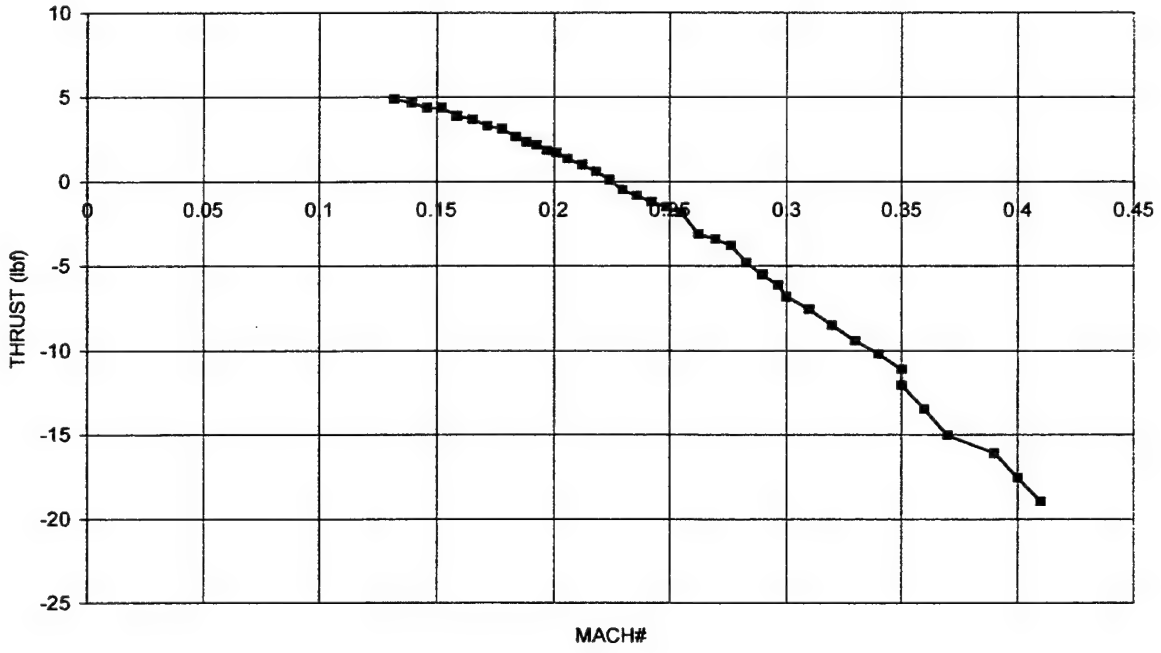

Figure 15. Subsonic Sea-Level Thrust Performance of the Shrouded Engine at 100% Spool Speed

3. Freejet on the Shrouded Engine Operating at 100%, 90%, 80% and IDLE RPM

The freejet was run at various supply pressures from the storage tanks. The starting value of pressure required was around 2.0 PSIG through the freejet exhaust nozzle. The required pressure was obtained by manually bumping open the valve to achieve the desired pressure. The engine was started and run up to 100% operating RPM while the starting air pressure value was achieved. As the air storage tanks were depleted the J450 operating RPM was set at 90%, 80% and IDLE. Two runs were completed to test repeatability. Pressure and force measurements were collected which are provided in Appendix C, Tables 12,13. Figure 16 is the Force vs Mach number.

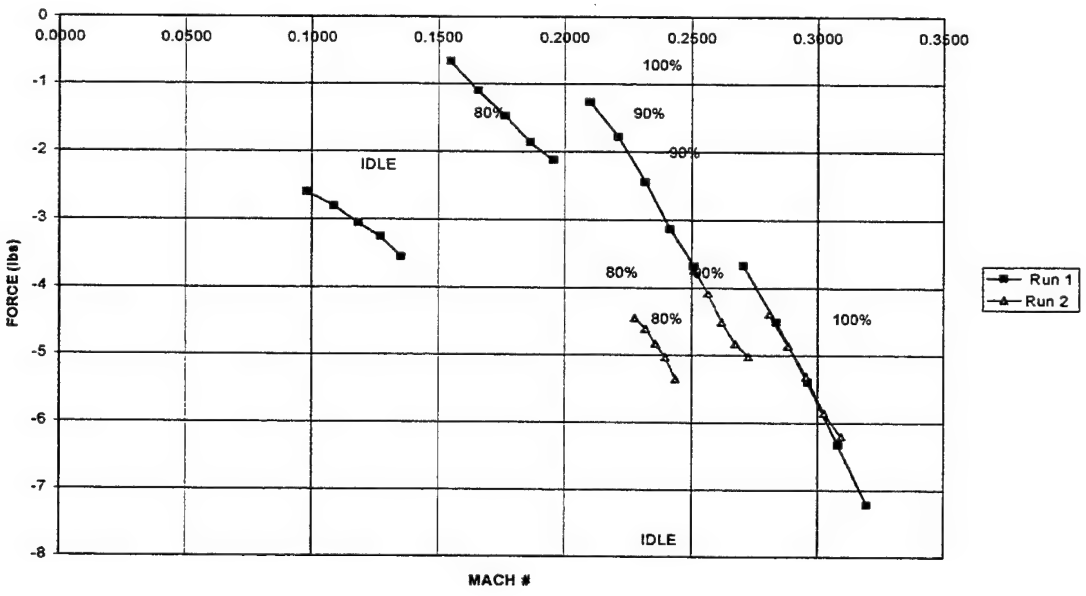

Figure 16. Performance Runs at Various Spool Speeds and Mach Numbers

4. Constant Mach # Performance of the Engine at Off-Design Conditions

The freejet was run with air supplied by the air compressor at a constant supply pressure. The constant value of pressure was .58 +/-.01 PSIG ahead of the freejet exhaust nozzle which produced a freejet Mach # of 0.235. The required pressure was obtained by running the air compressor at an exit pressure of 80 psia. The engine was started and run up to 100% operating RPM while the starting air pressure value was achieved. As the air compressor was operating the engine running RPM was set at 90%, 80% and IDLE. Pressure and force measurements were collected which are provided in Appendix C, Table 14. Figure 17 is the Force vs. Mach number.

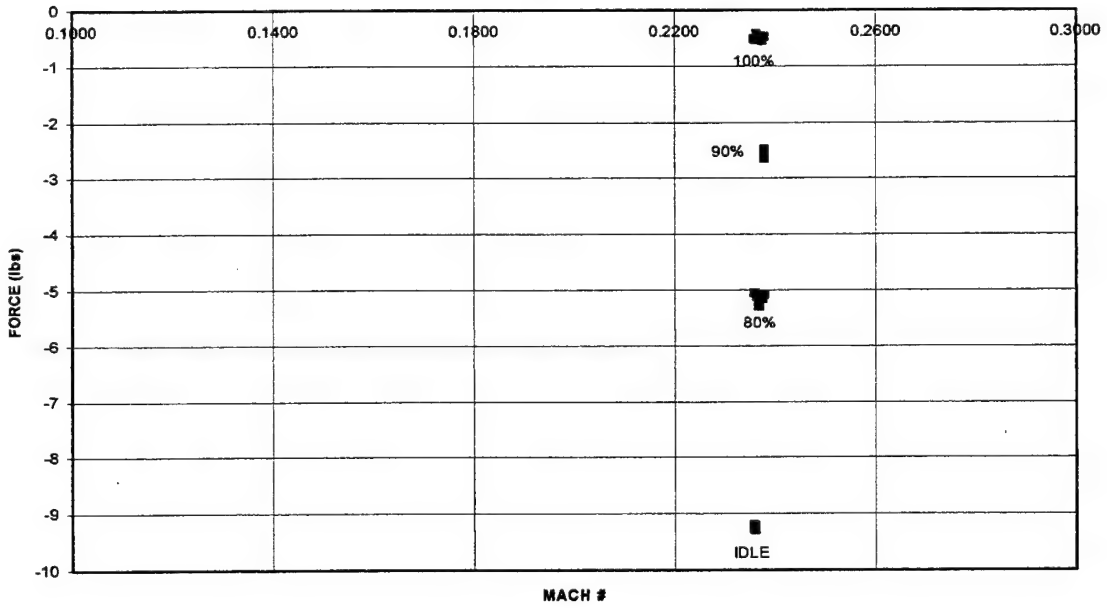

Figure 17. Constant Mach Number Performance of the Engine

5. Cycle Analysis Procedure of J450

The single spool turbojet design point analysis was selected once the GASTURB program was executed. The design point condition inputs to the program are provided below as Table 4. The design point speed being 115000 RPM.

The burner exit temperature was determined to be 1860 deg. R by using the iteration option of the software. Selecting the burner exit temperature as the iteration variable, and setting the net thrust determined from the J450 test program, 9.89 lbf, as the value to achieve, allowed the iteration algorithm of GASTURB to determine the necessary burner exit temperature. The design point calculated results are provided below as Table (5).

The off-design performance prediction involved the evaluation of the J450 at different spool speeds. The first step was to select the off-design option of GASTURB, then select the special map option. The SMOOTHC formatted compressor map for the Garrett T2 turbocharger (used in the J450) was selected during this analysis as was the default radial turbine map (RADTUR). The procedure for the use of GASTURB is provided in Appendix A.

The Garrett compressor map used in the GASTURB analysis is shown in Figure 18a, and the RADTUR turbine map is shown in Figure 18b. The speed lines were represented as fractions of the design speed [115000RPM]. Additionally, the figure has the predicted operating line of the engine displayed as squares while the circle on the [+0.994] speed line denoted the engine design point.

File: C: \PROGRA~1\OASTURB7\J450_2.CYJ
Date: Oct2000
Time: 12:01

Turbojet SL static, ISA

Basic Data		
Altitude	ft	0
Delta T from ISA	R	0
Mach Number		0
Inlet Corr. Flow W2Rstd	lb/s	0.256
Intake Pressure Ratio		1
Pressure Ratio		2.15
Burner Exit Temperature	R	1950
Burner Efficiency		1
Fuel Heating Value	BTU/lb	18.5
Rel. Handling Bleed		0
Overboard Bleed	lb/s	0
Rel. Overboard Bleed W_Bld/w2		0
Rel. Enthalpy of Overb. Bleed		0
Turbine Cooling Air W_Cl/W2		0
NOV Cooling Air W_Cl-NGV/w2		0
Power Of takes	hp	0
Mechanical Efficiency		1
Burner Pressure Ratio		1
Turbine Exit Duct Press Ratio		1
Nozzle Thrust Coefficient		1
Comp Efficiency		
Isentr . Compr Efficiency		0.653
Turb Efficiency		
Isentr.Turbine Efficiency		0.68

Table 4. GASTURB J450 Design Point Input Data

File: C:\PROGSA~1\CAsTURB7\J450_2.CYJ - modified
Date: Oct2000
Time: 10:57

Turbojet EL static, ISA

Station	W	T	P	WRstd		
amb		518.67	14.696		FN	9.89
2	0.256	518.67	14.696	0.256	TSFC	1.5703
3	0.256	699.62	31.596	0.138	FN/W2	1243.48
4	0.260	1860.00	31.596	0.229	Prop Eff	0.0000
41	0.260	1860.00		0.229	Core Eff	0.0974
5	0.260	1707.10	19.129	0.363	WF	0.0043
6	0.260	1707.10	19.129		WFRH	0.0000
8	0.260	1707.10	19.129		A8	1.2356
P2/Pi	= 1.0000	P4/P3 = 1.0000	P6/PS	= 1.0000	P8/Pamb	1.3016
Efficiencies:		isentr	polytr	RNI	Pwx	0
Compressor		0.7000	0.7301	1.00	W~NGV/W2	0.00000
Turbine		0.7100	0.6912	0.25	WC1/W2	0.00000
Spool	mech	1.0000			WB1d/W2	0.00000

Composed Values:
1: xM8 = 0.639225

Table 5. GASTURB Predicted Design Point Performance

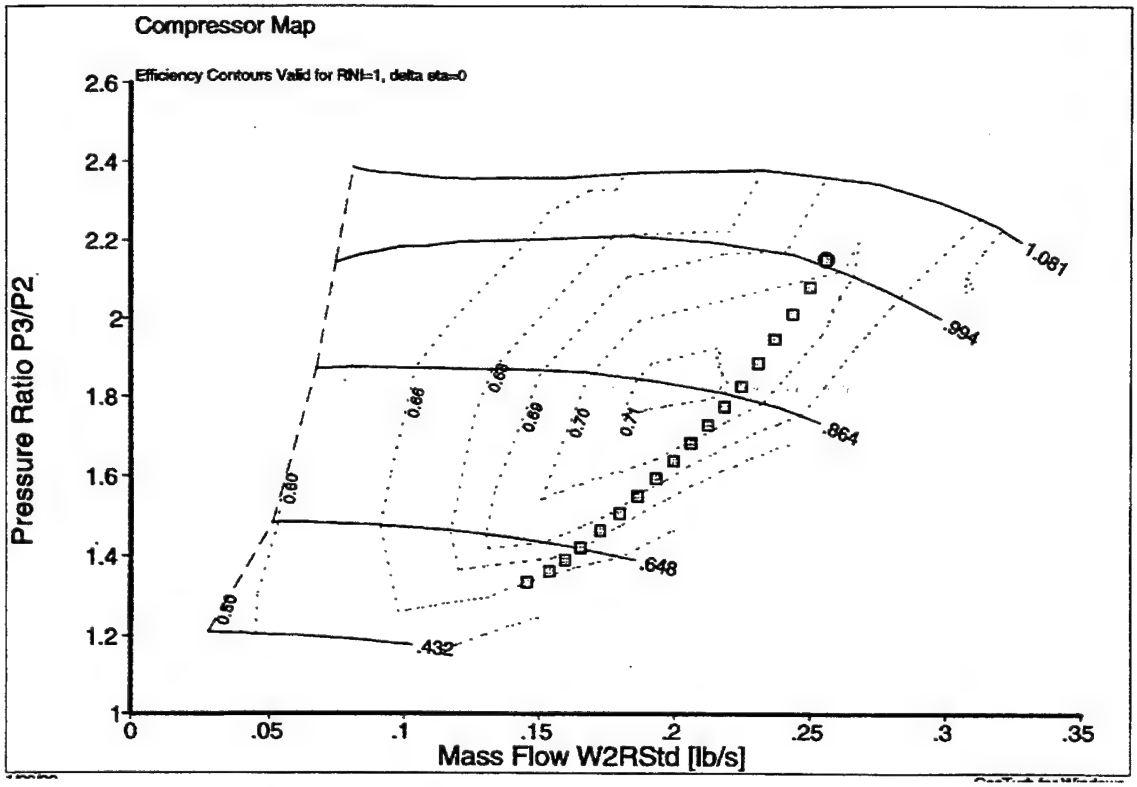

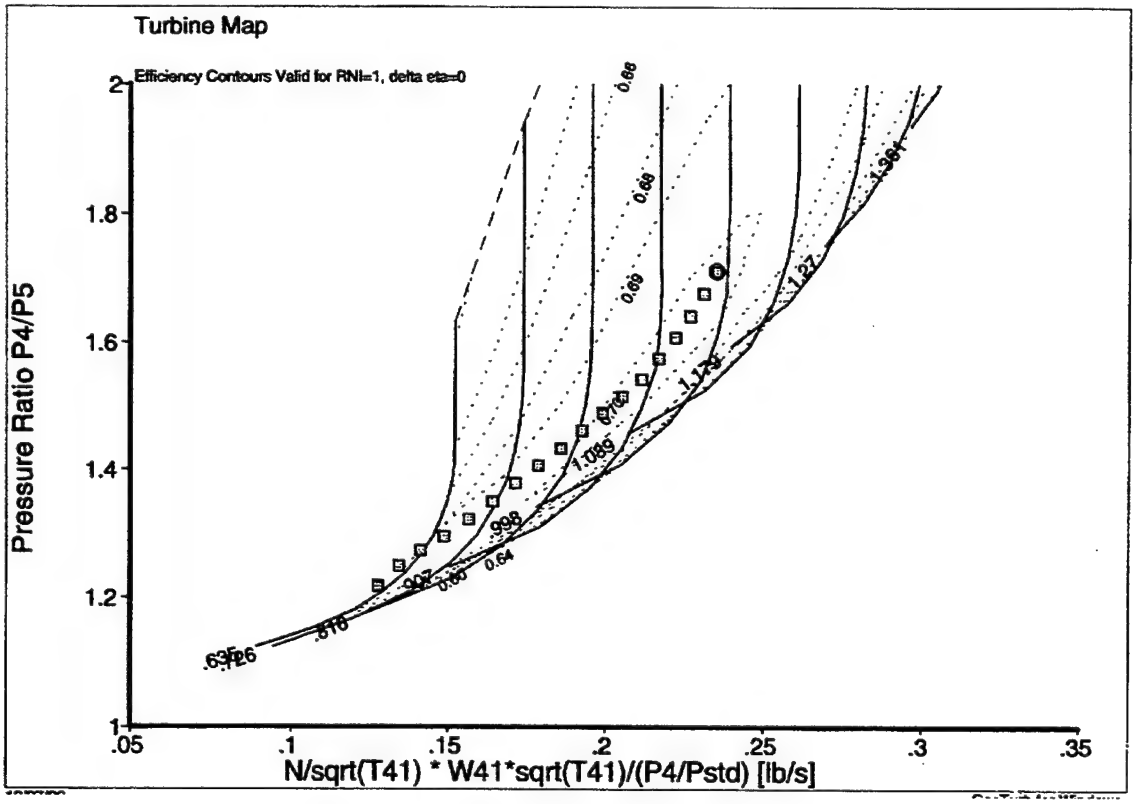

Figure 18a and 18b Compressor and Turbine Maps Respectively

F. SUMMARY AND COMPARISON OF FREEJET TEST RESULTS

1. Comparison of Predicted Drag and Thrust with Measurements of Shrouded J450 Drag and Thrust in Freejet

From Figure 19 predicted Drag, Thrust and Total Force were plotted from information obtained from GASTURB and correlations. Drag and Thrust measurements were taken from the engine operating at 100% RPM in the freejet operating at variable Mach numbers.

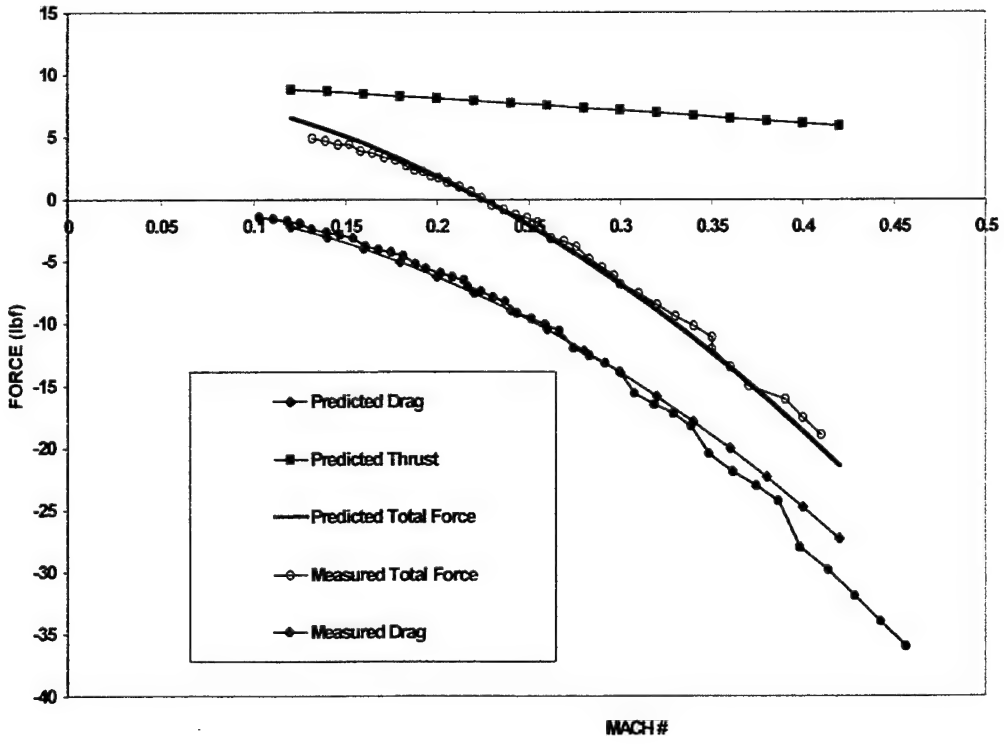

Figure 19. Comparison of Measured Results with Theory

2. Comparison of the Engine in Freejet with varying Mach # vs. a set Mach # of .23577

From Figure 20 three separate tests with the engine running at 100%, 90%, 80%, and Idle the measured total force were plotted. This was done to check the results to see if performance could be measured by operating the engine throughout the operating envelope at one set specific Mach number. This specific Mach number was chosen because it was the performance maximum of the freejet operating from the air compressor. This also happened to closely coincide with the cross-over performance point of the engine producing positive thrust in the dynamic environment.

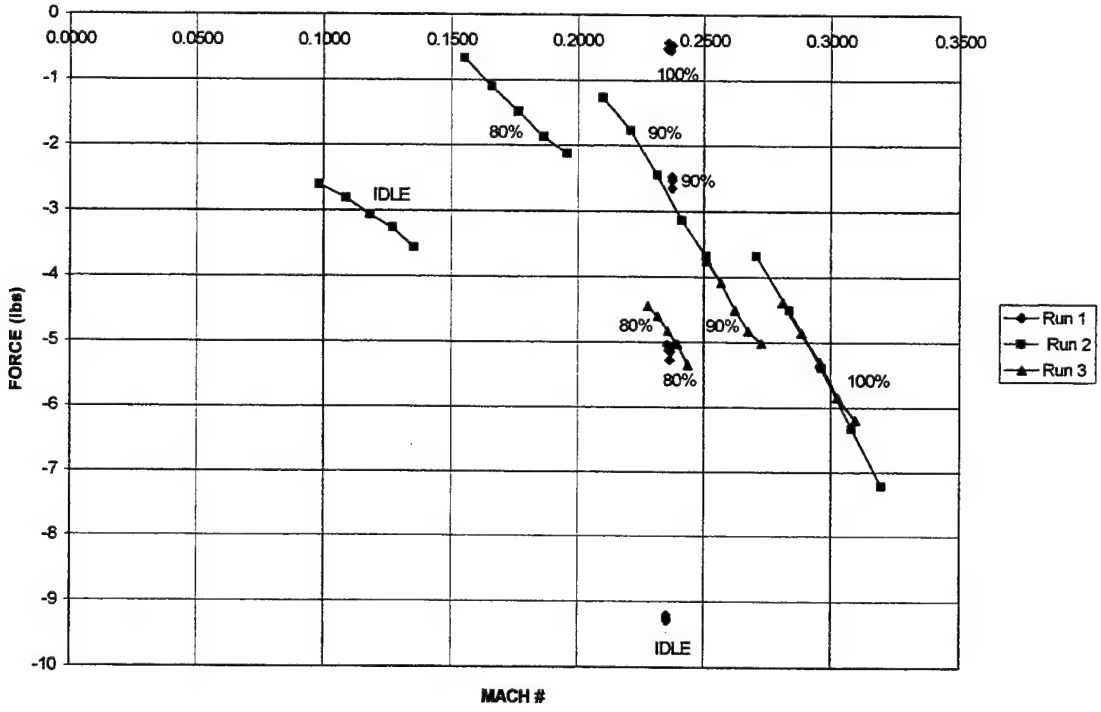

Figure 20. Comparison of Thrust with Varying Mach

III. COMPUTATIONAL FLUID DYNAMICS ANALYSIS

The advent of supercomputers has made possible the numerical solution of the Navier-Stokes equations applied to complex flows. Computational fluid dynamics (CFD) has been used in many aeronautical configurations of which there are numerous packages available. Many grid generation packages are also available for geometry and flow-field definition.

Creating a computational grid that accurately represents the object of study constitutes most of the effort involved in a CFD analysis, once a suitable flow solver has been developed. The grid generation procedure involves defining the solid geometry of the structure to be modeled, creating surface meshes that represent the object and finally incorporating these meshes into a grid block structure that encloses the object and surrounding free-stream space. Creating a single-block grid around a complex body while maintaining the required grid density and orthogonality is difficult.

NASA currently uses and supports a CFD code (OVERFLOW) which has extensively modeled the Space Shuttle vehicle aerodynamics (Ref. 7). The Naval Postgraduate School (NPS) has successfully applied OVERFLOW to single- and multi-block grid geometries at various flight conditions (Ref. 8).

A. GRIDGEN SOFTWARE DESCRIPTION

GRIDGEN is an interactive code used to generate three-dimensional grids around bodies, within user defined blocks. It can distribute grid points on curves, initialize and refine grid points on surfaces and initialize volume grid points. GRIDGEN Version 9,

sponsored by NASA Ames Research Center (ARC) and developed by Computer Sciences Corporation, was written using the Silicon Graphics Iris GL graphics library and runs on Silicon Graphics 4D Series and IBM RS/6000 Series workstations. (Ref. 9)

GRIDGEN is not a computer aided design (CAD) package and as such does not have the tools to define complex geometries but can generate simple three-dimensional and most two-dimensional shapes. The first step in grid generation is to either draw the object in a CAD package and import it into GRIDGEN or generate the required shapes directly. The only purpose of the CAD surface generation is to define the object and this usually has no relationship to the grid topology or quantity of grid points.

B. GRID GENERATION PROCESS

Creating a volume grid in GRIDGEN requires following a set of successive steps that include:

* defining the outer boundaries of the grid by creating a series of continuous segments, called connectors, which have grid points defined and distributed along their length,
* generating a four edged mesh called a domain, which is smoothed using algebraic or elliptic smoothing routines, and
* grouping the domains together to form a viable computational block and smoothing the final three-dimensional volume grid.

1. Connector Description

Connectors consist of line and curve segments that form the outer boundary structure of the grid. Each connector begins and ends with a control point and may consist of several sub-connectors.

Segments within a connector are dimensioned and grid points are distributed along the segment. Grid point locations are controlled by geometric or linear distribution functions. Specific controls are available to dictate exact grid point spacing parameters.

2. Domain Description

A domain is a surface mesh defined by four edges. Each edge consists of one or more connectors joined through control points. The quantity of grid points on each edge forming a domain must match its opposite edge. There are no limits on the size of the domains; however the domain shape will affect the contours of the final volume grid.

C. RESULTS OF GRIDGEN

A two-dimensional grid was constructed and rotated axi-symetrically about the X-axis of the intake cone to produce a three-dimensional grid as in Figure 21. The intake is modeled as a 15° cone extending three diameters outside the intake lip. The intake cowl was canted inward towards the flow by 4.6 degrees. This angle was the theoretical flow turning angle after the external oblique shock (Ref. 6).

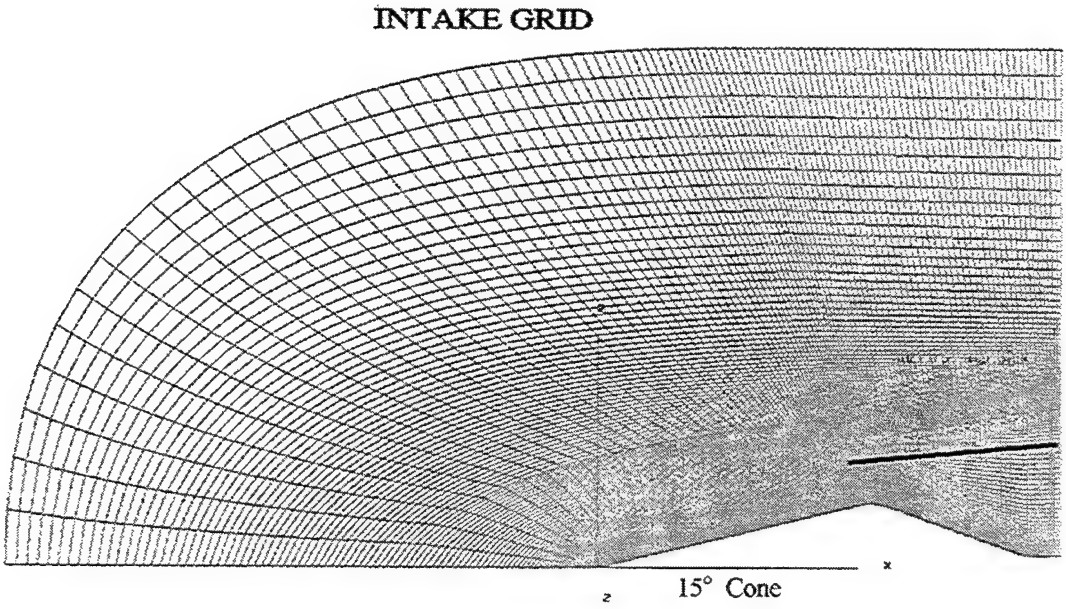

Figure 21. Intake Grid

D. OVERFLOW SOFTWARE DESCRIPTION

OVERFLOW is an implicit flow-solver which was written and developed at NASA ARC. The code solved the Reynolds-Average Navier-Stokes (N-S) equations in strong conservative form, and the initial boundary conditions to compute the flow solution. User controlled parameters included:

1. basic flow properties such as the angle-of-attack, sideslip angle, Reynolds number, free-stream Mach number;

2. variations in the properties of the ratios of specific heats;

3. solution controls such as time stepping, stability parameters, differencing schemes and smoothing;

4. boundary conditions applied to symmetry planes, outer grid boundaries, solid surfaces, C-grid "cuts"; and

5. turbulence model types which include Baldwin-Lomax boundary and shear layer models and the Baldwin-Barth one equation model and k-w two equation model (used in this study).

E. OVERFLOW ANALYSIS

The flow analysis over the supersonic inlet was computed first with an inviscid (Euler) and then a viscid (N-S) analysis. This approach provided immediate feedback on the symmetry of the grid and validity of the input file boundary conditions. The Overflow input file for the viscous solution is attached as Appendix G.

1. Input Conditions

The Euler and Navier-Stokes solutions were initiated by treating the body surface as either an inviscid or viscous adiabatic wall. The free-stream flow was initialized at a Mach number of 2.0 and a Reynold's number of 1.67×10^5 .

F. RESULTS OF OVERFLOW

Overflow produced a solution file, q.save, a residual file, resid.out, and a force and moment file, fomo.out, which were required to evaluate the CFD model. The solution file was run using 14,000 iterations. The solution was checked for convergence by ensuring the residual (or L_2 norms) of the density had decreased by at least two orders of

magnitude. From the Mach # representation of the solution file, Figure 22, it was (of the cone-only solution), able to measure the oblique shock angle. Mach number distributions throughout the two shock system Figure 23 and static pressure fields Figure 24 were displayed with FAST. The supersonic flow field can be seen in Figure 25.

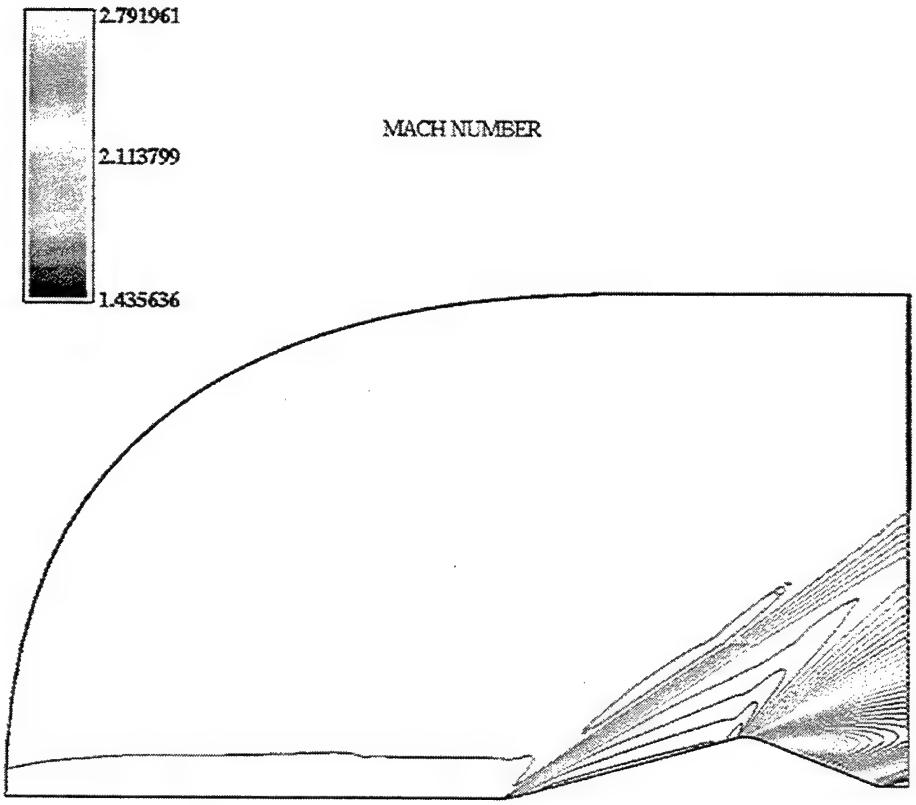

Figure 22. Invisid Mach # Flow Field for Cone Only

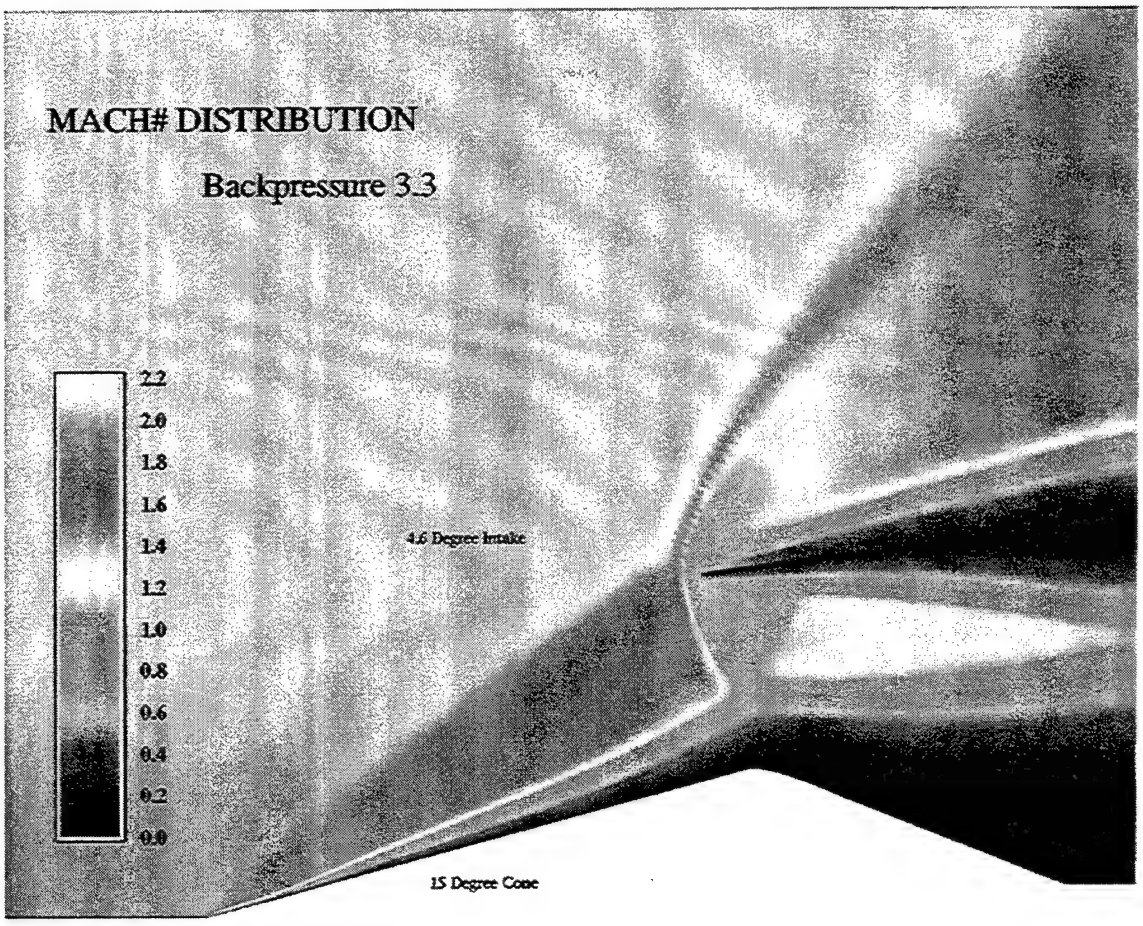

Figure 23. Mach # Distribution in Supersonic Intake

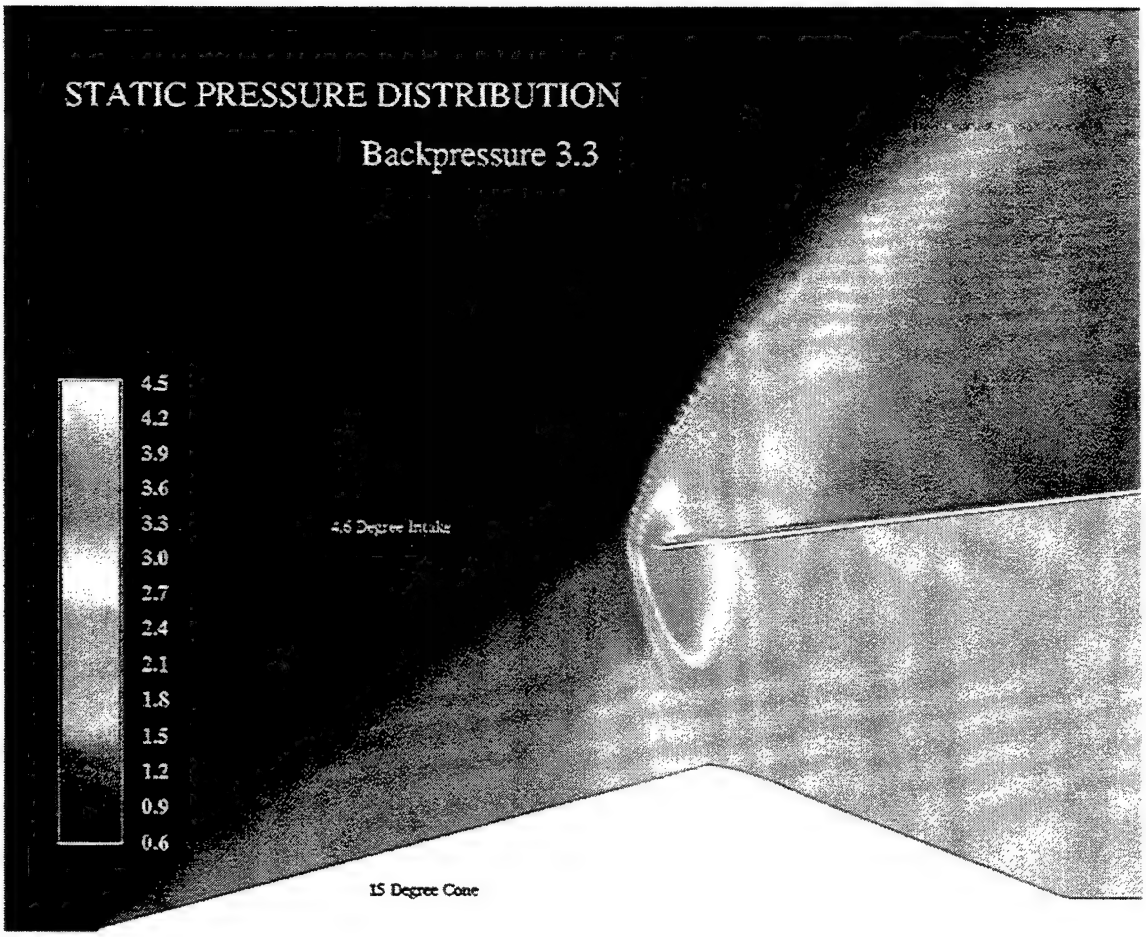

Figure 24. Static Pressure Distribution in Supersonic Intake

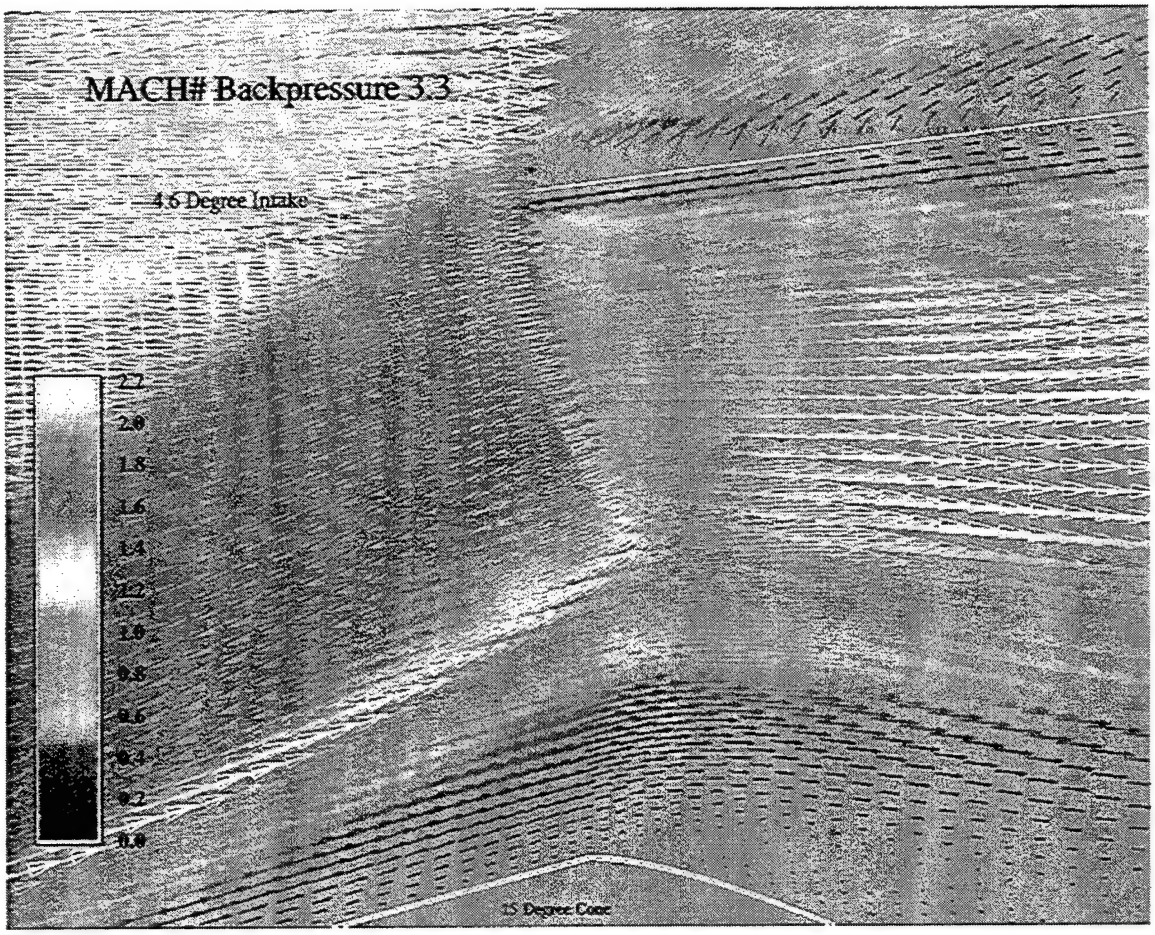

Figure 25. Mach 2 Supersonic Flow Field

G. RESULTS AND COMPARISONS OF COMPUTATIONAL FLUID DYNAMICS

Conical shock theory for a 15 degree cone in a free stream Mach number of 2 will yield an oblique shock angle of 33.9 degrees (Ref. 6). The oblique shock angle in the solution is well within the 33-35 degree range for the inviscid cone only solution. The addition of the outer inlet cowl, along with changing the parameters to a viscid solution, necessitated the canting of the intake 4.6 degrees. This coincided with the theoretical calculation of the actual inlet design (Ref. 6). A back-pressure of 3.3 (times free-stream pressure) was placed at the exit boundary inside of the engine shroud. This was to simulate the back-pressure created by the engine. This is the amount of back-pressure required to produce the desired placement of the second normal shock in the inlet.

IV. CONCLUSIONS AND RECOMMENDATIONS

A. CONCLUSIONS

A new freejet facility was constructed, along with a new engine stand for the Naval Postgraduate School. This new facility allowed for the dynamic subsonic testing of a shrouded turbojet engine. The initial dynamic testing was another successful milestone to produce a combined cycle engine (CCE).

The dynamic testing allowed for actual limited flight conditions up to the speed of Mach .4 to be produced. These conditions allowed the measurement of performance parameters such as thrust, specific fuel consumption and drag. These performance measurements produced superior results when compared with the performance prediction software GASTURB. The freejet facility allowed for many successful runs with outstanding repeatability of results.

Along with the dynamic subsonic testing of the shrouded inlet, the supersonic regime of the inlet design was analyzed with computational fluid dynamics. The inlet design was proven to be successful and closely matched the theoretical predictions. Some minor enhancements to the original inlet design point were made which allowed for increased performance with correct positions of the shocks in the intake.

The initial testing and design of the afterburning fuel dispersion section of the ramjet were initiated which would successfully complete the combined cycle or turborambjet engine.

B. RECOMMENDATIONS

To continue with the freejet facility improvements by the installation of a valve, which would allow to more precisely regulate the flow of air through the freejet exhaust nozzle. The exhaust pipe for the freejet and engine needs to be turned upwards to deflect the flow of air and silence the facility.

With the possible predicted increase in performance of the CCE and probable higher subsonic Mach number testing. It will be necessary to add an additional thrust beam to the engine stand. This would assist in the stabilization of the engine and also allow the continued collection of quality data.

The afterburning portion of the scramjet needs to be further developed and tested in the freejet to be successful as a combined cycle engine.

The computational fluid dynamics portion of the CCE analysis can be furthered by modeling the entire engine and using OVERFLOW to predict the flow dynamics/characteristics at the design Mach number 2.0 and higher.

APPENDIX A. GASTURB (OFF-DESIGN PERFORMANCE)

Process: Perform a single cycle calculation for a single spool turbojet by selecting **[calculate Signal Cycle]** and press **[Go On]**. For the initial calculation you most enter the engine type, at the prompt select **[Sophia]** or select the **[demo-jet.cyj]** and enter the data contained in at the end of this process as Table 4, into the Design Point Input menu. When complete selected **[Go On]**, the design Turbojet SL and static performance should appear as indicated in Table 5. Press **[Close]** twice to perform off design calculations. Once at the introduction screen, select [Off Design] and then select **[Go On]**. At this point select **[Maps]**, to read in special compressor and or turbine maps. Select **[Maps]** then [Special], the special component map screen will appear. Select **[Read]** to read special compressor or turbine into the current file.**[Compr or Turb]** must be selected after the map is read into the current file to view and select the design point with the small yellow square. By placing the pointer over the yellow square (design point) and press the right mouse button to move the design point to coincide with experimental data. Once both the compressor and turbine maps are selected and the design points verified **[Close]** the component map window.

To create an operating line selects **[Task]** and choose [Line] **operating** and **[Go On]** Increase the number of points in the operation line to **[20]**. Select the down arrow for decreasing load and select **[go on]** once computed, select no for another operation line. You can now elect to view pressure ratio Vs mass flow rate or a variety of many other combinations. Or you can select to view operation line of the **[Compressor or Turbine]** once complete Select **[Close]** once to return to the off-design-input screen. If you wish to Compare other turbine map combination select Maps and repeat the steps from that point to continue analysis. If you finished with comparisons continue to select **[Close]** until the startup screen to exit.

THIS PAGE IS INTENTIONALLY LEFT BLANK

APPENDIX B. CALIBRATION DATA

DATE: 10/26/2000

FUEL CELL CALIBRATION

VOLTS (mV)	WEIGHT (lbs.)
0	0
.019	.5
.0378	1.0
.0928	2.5
.1106	3
.1284	3.5
.1459	4
.1811	5

Table 6. Fuel Cell Calibration

THRUST BEAM CALIBRATION

VOLTS (mV)	WEIGHT (lbs.)
-1.002	-13.25
-0.615	-8.25
0	0
0.659	8.25
1.058	13.25

Table 7. Thrust Beam Calibration

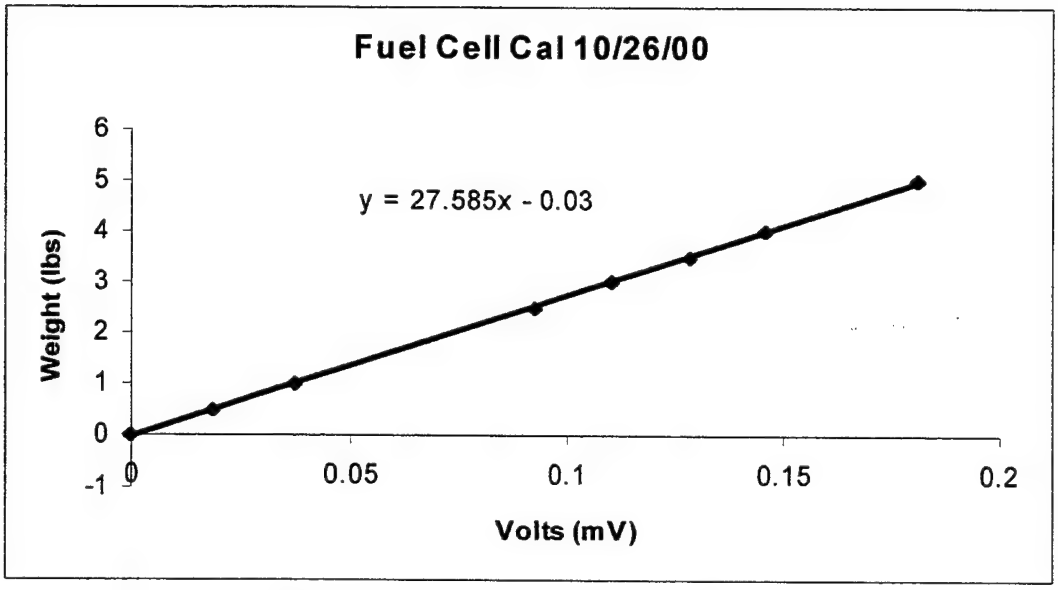

Figure 26. Fuel Cell Calibration

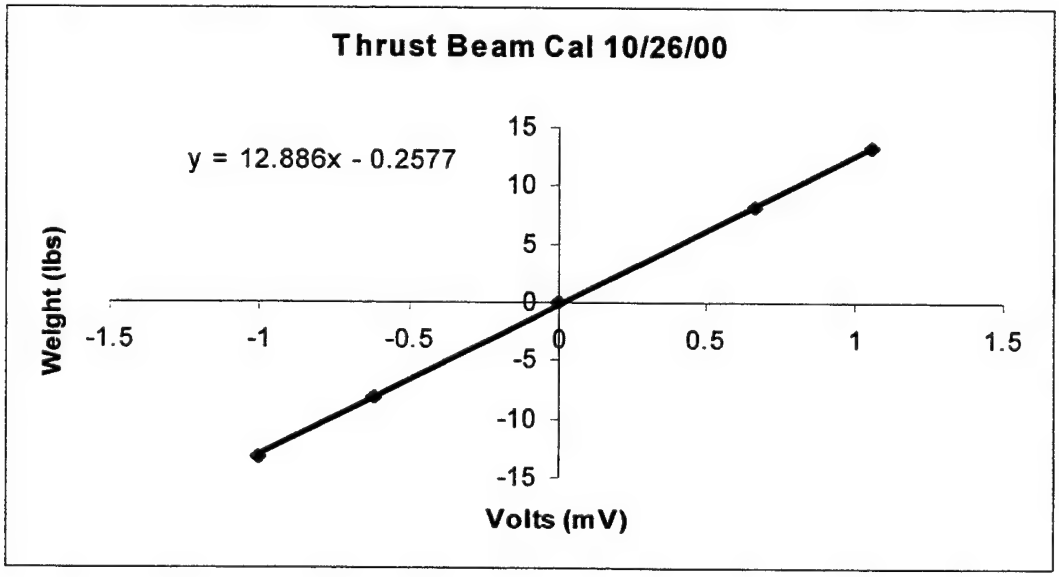

Figure 27. Thrust Beam Calibration

APPENDIX C. ENGINE TEST RESULTS

REFERENCED MATERIAL

TABLE 8

ELLIPTICAL INTAKE

MEDIUM SHROUD

RUN @ 105% RPM	THRUST (lbf)	FUEL FLOW (lb/sec)
1	9.405	.00513
2	9.384	.00503
3	9.414	.00511
4	9.472	.00501
AVERAGE	**9.419**	
RUN @ 100% RPM		
1	8.420	.00453
2	8.422	.00455
3	8.450	.00456
4	8.401	.00459
AVERAGE	**8.423**	
RUN @ 90% RPM		
1	6.551	.00368
2	6.531	.00368
3	6.516	.00380
4	6.535	.00370
AVERAGE	**6.533**	
RUN @ 80% RPM		
1	4.257	.00287
2	4.216	.00289
3	4.250	.00289
4	4.237	.00298
AVERAGE	**4.24**	

DATE: 09/22/00

TABLE 9

INTAKE REMOVED

RUN @ 105% RPM	THRUST (lbf)	FUEL FLOW (lb/sec)
1	10.8022	.004758
2	10.8199	.004797
3	10.8498	.004751
4	10.9001	.004714
AVERAGE	**10.8448**	**.004755**
RUN @ 100% RPM		
1	9.4897	.0041904
2	9.50186	.0042139
3	9.5450	.0042188
4	9.5645	.0041327
AVERAGE	**9.5320**	**.0041889**
RUN @ 90% RPM		
1	7.7742	.0034532
2	7.8254	.0034931
3	7.7975	.0035703
4	7.7769	.0034522
AVERAGE	**7.787**	**.0034922**
RUN @ 80% RPM		
1	5.4424	.0027114
2	5.4541	.0027208
3	5.4586	.0026901
4	5.4468	.0027108
AVERAGE	**5.4497**	**.002708**
RUN @ IDLE		
1	2.7551	.0017623
2	2.7820	.0018347
3	2.8278	.0018881
4	2.8156	.0019368
AVERAGE	**2.7999**	**.0018555**

DATE: 09/22/00

TABLE 10

CONICAL INTAKE

RUN @ 105% RPM	THRUST (lbf)	FUEL FLOW (lb/sec)
1	9.40649	.0047495
2	9.42604	.0048015
3	9.46241	.0047120
4	9.4789	.0046996
AVERAGE	**9.4525**	**.004741**
RUN @ 100% RPM		
1	8.15167	.0041853
2	8.20639	.0041558
3	8.17784	.0041478
4	8.20012	.0041024
AVERAGE	**8.1775**	**.0041478**
RUN @ 90% RPM		
1	6.54528	.0034726
2	6.53625	.0035369
3	6.52672	.0034911
4	6.53217	.0035389
AVERAGE	**6.5341**	**.0035099**
RUN @ 80% RPM		
1	4.17061	.0027095
2	4.16873	.0026580
3	4.17366	.0026991
4	4.16111	.0026734
AVERAGE	**4.1753**	**.0027001**
RUN @ IDLE		
1	1.60299	.001934
2	1.16436	.001916
3	1.60095	.001919
4	1.5914	.001909
AVERAGE	**1.60765**	**.001919**

TABLE 11

DATE: 10/26/00

DATE: 10/19/00

A. FREEJET ON NON-RUNNING ENGINE			B. ENGINE OPERATING AT 100% IN FREEJET	
THRUST	MACH #		THRUST	MACH #
-36.04	0.4566		-18.95	0.41
-34.02	0.4429		-17.56	0.4
-31.92	0.4287		-16.11	0.39
-29.85	0.4139		-15.04	0.37
-28	0.3985		-13.5	0.36
-24.26	0.3867		-12.07	0.35
-23.06	0.3746		-11.12	0.35
-21.91	0.3619		-10.2	0.34
-20.46	0.3487		-9.41	0.33
-18.29	0.339		-8.5	0.32
-17.21	0.3291		-7.56	0.31
-16.49	0.3188		-6.82	0.3
-15.62	0.308		-6.12	0.2965
-13.88	0.3		-5.5	0.2898
-13.18	0.2918		-4.8	0.2829
-12.57	0.2833		-3.8	0.2761
-11.97	0.2745		-3.4	0.2693
-10.6	0.2671		-3.1	0.2622
-10.07	0.2595		-1.85	0.2549
-9.63	0.2517		-1.5	0.2489
-9.17	0.2436		-1.22	0.2426
-8.21	0.2372		-0.83	0.2362
-7.86	0.2307		-0.5	0.2296
-7.4	0.2239		0.094	0.2239
-7.02	0.2169		0.604	0.218
-6.5	0.2147		0.99	0.2119
-6.25	0.2086		1.34	0.2057
-5.94	0.2022		1.7	0.201
-5.6	0.1944		1.85	0.1968
-5.2	0.1888		2.2	0.1925
-4.57	0.1823		2.35	0.1881
-4.25	0.1757		2.68	0.1836
-4.03	0.1687		3.15	0.1776
-3.78	0.1615		3.33	0.1715
-3.16	0.1546		3.7	0.1651
-2.85	0.1475		3.89	0.1584
-2.68	0.1399		4.39	0.1522
-2.41	0.1319		4.38	0.1458
-1.99	0.1254		4.68	0.139
-1.76	0.1185		4.9	0.1319
-1.59	0.1111			
-1.46	0.1033			

DATE: 10/19/00

TABLE 12

ENGINE OPERATING AT 100%, 90%, 80%
AND IDLE IN VARIABLE MACH # FREEJET

RUN 1 @ 100% RPM	FORCE (lbf)	MACH #
1	-7.22165	0.3199
2	-6.33558	0.3084
3	-5.39782	0.2965
4	-4.5118	0.2841
5	-3.68179	0.2710
RUN 1 @ 90% RPM		
1	-3.68648	0.2513
2	-3.13818	0.2417
3	-2.44919	0.2317
4	-1.78247	0.2213
5	-1.27458	0.2103
RUN 1 @ 80% RPM		
1	-2.12827	0.1962
2	-1.87893	0.1869
3	-1.48733	0.1770
4	-1.1091	0.1666
5	-0.67517	0.1554
RUN 1 @ IDLE		
1	-3.56367	0.1356
2	-3.26632	0.1273
3	-3.06986	0.1185
4	-2.81482	0.1089
5	-2.61027	0.0985

DATE: 10/19/00

TABLE 13

ENGINE OPERATING AT 100%, 90% AND 80%

IN VARIABLE MACH # FREEJET

RUN 2 @ 100% RPM	FORCE (lbf)	MACH #
1	-6.20304	0.3096
2	-5.85684	0.3027
3	-5.31259	0.2958
4	-4.86114	0.2886
5	-4.38895	0.2812
RUN 2 @ 90% RPM		
1	-5.01776	0.2728
2	-4.82885	0.2676
3	-4.50549	0.2623
4	-4.09221	0.2568
5	-3.74506	0.2513
RUN 2 @ 80% RPM		
1	-5.35395	0.2436
2	-5.03657	0.2397
3	-4.82759	0.2358
4	-4.60919	0.2317
5	-4.45064	0.2276

DATE: 10/19/00

TABLE 14

ENGINE OPERATING AT 100%, 90%, 80%

AND IDLE AT A STATIC MACH # OF .23577 FREEJET

100% RPM	**FORCE (lbf)**	**MACH #**
1	-0.52137	0.2358
2	-0.43266	0.2363
3	-0.50629	0.2368
4	-0.54675	0.2373
5	-0.47279	0.2378
90% RPM		
1	-2.53097	0.2378
2	-2.47865	0.2378
3	-2.65034	0.2378
4	-2.51058	0.2378
5	-2.64565	0.2378
80% RPM		
1	-5.08355	0.2378
2	-5.15311	0.2373
3	-5.28344	0.2368
4	-5.12427	0.2363
5	-5.04977	0.2358
IDLE		
1	-9.24784	0.2358
2	-9.27259	0.2358
3	-9.20491	0.2358
4	-9.27761	0.2358
5	-9.28795	0.2358

THIS PAGE IS INTENTIONALLY LEFT BLANK

APPENDIX D. ENGINE TEST PROGRAM CHECKLIST

D1. FUEL WEIGHT AND THRUST BEAM CHECKLIST

D2. DATA ACQUISITION SYSTEM SETUP CHECKLIST

D3. DATA ACQUISITION SYSTEM CHECKLIST

D4. DATA PURGE CHECKLIST

D1. FUEL WEIGHT AND THRUST BEAM CALIBRATION

1. Ensure that the test rig is configured in accordance with Figures # and # of [Ref. 1] and that all devices are properly energized.

2. The-fuel pump power supply should be [**OFF**] with the voltage knob turned counter clockwise until slight resistance is felt.

3. Zero the thrust beams by connecting the **CHANNEL [6]** output of the signal condition to the DVM front panel, HI/LOW on right side. Once properly connected, adjust the **ZERO KNOB** accordingly until the DVM reads 0 mV. Apply loads to the engine and record voltage. Once calibrated, restore the signal conditioner and DVM to their initial configuration (REAR position)

4. *Calibrate the fuel flow beam in the following manner*.

   4.1 Connect the strain gages **[1 and 2]** in a half Whetstone bridge configuration as shown on the inside cover of the P3500.

   4.2 Set the bridge push button to **half-bridge** position.

   4.3 Depress AMP ZERO and adjust thumb wheel until [**±000**] is displayed.

   4.4 Depress GAGE FACTOR and ensure the range is set on [**1.7-2.5**].

   4.5 Adjust GAGE FACTOR knob until [**2.080**] is displayed.

   4.6 Depress RUN and set the BALANCE Control for a reading of [**±000**].

   4.7 With a DVM connected to the P3500 output, adjust the OUTPUT thumb wheel until the DVM reads [**0 mV**].

   4.9 Perform a calibration of Fuel weight

   4.8 Disconnect the external **DVM.**

5. Place Fuel bottle on carriage and connect fuel line to engine.

6. Prime fuel pump by disconnecting the fuel line forward of the check valve.

D2. DATA ACQUSITION SYSTEM SETUP

1. Energize the HP9000 computer system.

2. The first screen is the HP9000 Series 300 Computer Data Acquisition /Reduction System introduction.

3. Select **[F7]** and set the current time and date The format is **HH: MM: SS** for the time, then select **[F2]** and set the date **DD MMM YYYY**, (i.e. **10:20:00,08 Jan 2000**)

4. Press **Shift** and then **Reset** at same time .

5. Type **CAT** and then return.

6. Type **MSI "HP6944AOLD"** then return.

7. Press **[F5]** then type "**Thrust_SFC**" then return.

8. Type **LIST** then return.

9. Press **[F1]** then return.

10. Go to line **[210]** then change the value of the Fuel weight calibrated then return.

11. Go to line **[370]** then change the value of the thrust calibrated then return.

12. Press **Shift** and then **Reset** at same time.

13. Press **[F8]** then type "**Thrust_SFC**" then return.

14. Press **[F3]** to **RUN** the program.

15. Type "printer is **702"** for using the printer.

16. Type "printer is **CRT"** to go back to the screen.

The program is attached at Appendix [E].

D3. DATA ACQUISITION SYSTEM

1. Energize the Nitrogen system and select **[F4]**.

2. Once the engine is operating at the desired speed and stabilized, select **[F5]** to begin data acquisition sequence.

3. Manually record the Thrust and Fuel Flow rate for each of the data runs as displayed on the screen.

4. Once the data collection sequence is completed, secure the engine

5. Secure Nitrogen once post calibration is complete

6. Select **[F6]** to begin data reduction.

7. Select [**F8**] to exit once data reduction is complete.

8. Select [**STOP**] to display the reduced data.

9. Select [**F5**] and type "READ-MJ-ZOC".

10. Select [**F3**] to RUN.

11. Enter **1,** date (YMMDD), Run number (i.e. for run 1 **on** 10 Jan 2000, type:1,90308,1).

12. Select [**1**] for printer option.

13. Select [**0**] to Exit.

NOTE: Selecting exit does not exit the program but displays the average of the port readings for the selected data run.

14. Select [**STOP**] to exit the program.

15. Repeat steps 10-13 for the remaining data **runs.**

16. If ejector data was measured select [**STOP**].

17. Select [**F5**] and type "EJ_ZOC"

18. Select [**F3**] to run.

19. Data files are presented in the same manner as above.

20. When complete viewing data select [**STOP**].

21. Type "printer is **CRT**"

D4. DATA FILE PURGE

1. The raw data files are stored on the **"HP9000":,700"** hard drive as ZW190381 (example for 19 Nov 2000, run number 1) through ZW19038X for X data runs.
2. The reduced data files are stored as ZRXXXXXX and the calibration data is stored as ZCXXXXXX.
3. Select [**F5**] and type "ZOC_MENU".
4. Select [**F3**] to Run.
5. Select [**F8**] to exit menu.
6. Type [**MSI":700"**].
7. Type [**PURGE"FILENAME"**]. (eg PURGE "ZW190381").
8. Ensure deletion of each files. If all created files are not deleted an error will be encountered if obtaining additional data.
9. Cycle the power switch on the lower left corner of the HP9000 CPU to reset the computer.

THIS PAGE IS INTENTIONALLY LEFT BLANK

APPENDIX E. STRAIN GAGING

PURPOSE: The thrust and fuel consumption of the engine were measured by beams from which the engine and fuel tank were suspended. The beams were configured with strain gages, the engine thrust beam with four gages [two one each side] and the fuel beam with two [one on each side]. The thrust beam strain gages were configured in a full Whetstone bridge. On the fuel beam set-up a half bridge was incorporated. Figure (28) depicts the wiring code for the Thrust beam configuration. The following text refers to actual strain gage attachment. Figure (29) depicts a strain gage located on the fuel beam.

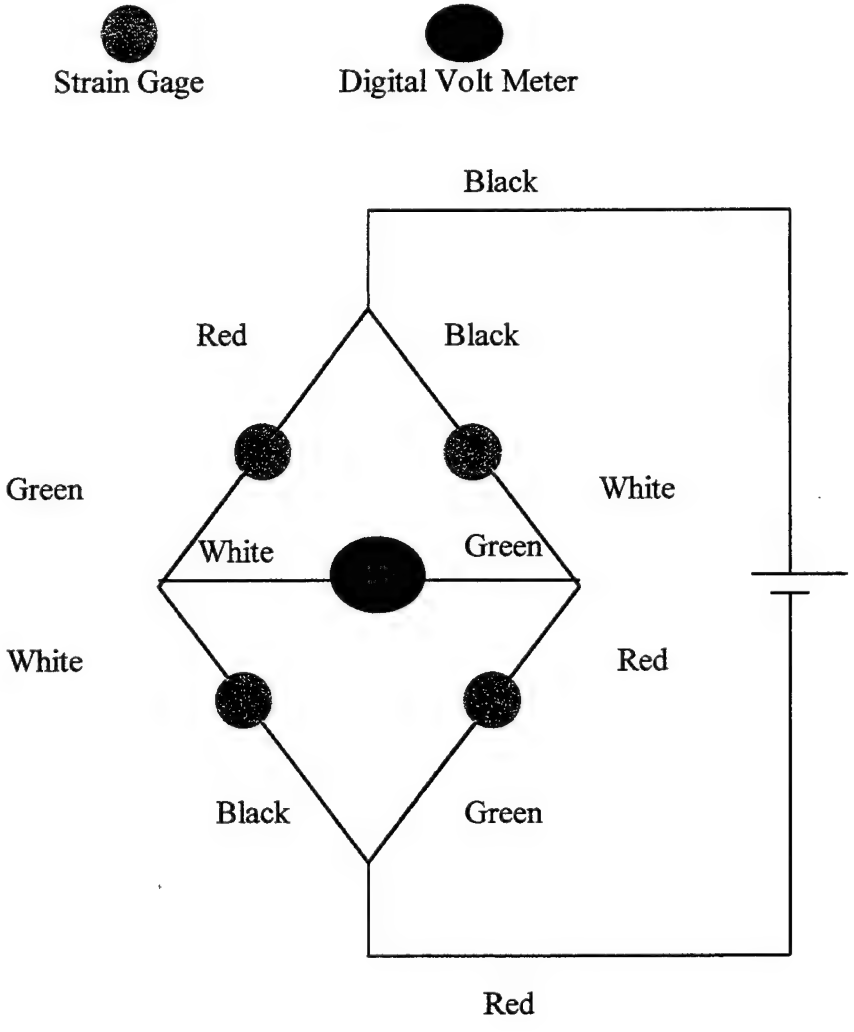

Figure 28. Wiring Code for Thrust Beam Full Whetstone Bridge

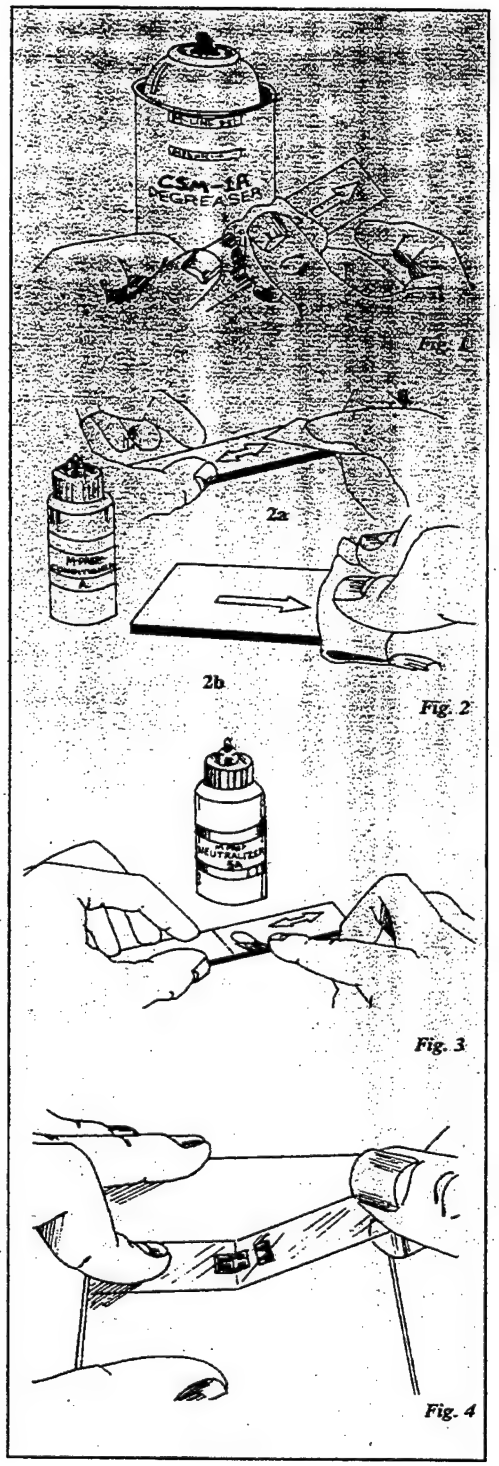

Fig. 1

Fig. 2

Fig. 3

Fig. 4

GAGE APPLICATION TECHNIQUES

The installation procedure presented on this and the following pages is somewhat abbreviated and is intended only as a guide in achieving proper gage installation with M-Bond 200. *Micro-Measurements Instruction Bulletin B-129* presents recommended procedures for surface preparation, and lists specific considerations which are helpful when working with most common structural materials.

Step 1

Thoroughly degrease the gaging area with solvent, such as CSM-1A Degreaser or GC-6 Isopropyl Alcohol (Fig. 1). The former is preferred, but there are some materials (e.g., titanium and many plastics) which react with chlorinated solvents. In these cases GC-6 Isopropyl Alcohol should be considered. All degreasing should be done with uncontaminated solvents — thus the use of "one-way" containers, such as aerosol cans, is highly advisable.

Step 2

Preliminary dry abrading with 220- or 320-grit silicon-carbide paper (Fig. 2a) is generally required if there is any surface scale or oxide. Final abrading is done by using 320- or 400-grit silicon-carbide paper on surfaces thoroughly wetted with M-Prep Conditioner A; this is followed by wiping dry with a gauze sponge. Repeat this wet abrading process, then dry by slowly wiping through with a gauze sponge, as in Fig. 2b.

With a 4H pencil (on aluminum) or a ballpoint pen (on steel), burnish *(do not scribe)* whatever alignment marks are needed on the specimen. Repeatedly apply M-Prep Conditioner A and scrub with cotton-tipped applicators until a clean tip is no longer discolored. Remove all residue and Conditioner by again slowly wiping through with a gauze sponge. Never allow any solution to dry on the surface because this invariably leaves a contaminating film and reduces chances of a good bond.

Step 3

Now apply a liberal amount of M-Prep Neutralizer 5A and scrub with a cotton-tipped applicator. See Fig. 3. With a single, slow wiping motion of a gauze sponge, carefully dry this surface. Do not wipe back and forth because this may allow contaminants to be redeposited.

Step 4

Using tweezers to remove the gage from the transparent envelope, place the gage (bonding side down) on a chemically clean glass plate or gage box surface. If a solder terminal is to be incorporated, position it on the plate adjacent to the gage as shown. A space of approximately 1/16 in *(1.6 mm)* should be left between the gage backing and terminal. Place a 4- to 6-in *(100- to 150-mm)* piece of Micro-Measurements No. PCT-2A cellophane tape over the gage and terminal. Take care to center the gage on the tape. Carefully lift the tape at a shallow angle (about 45 degrees to specimen surface), bringing the gage up with the tape as illustrated in Fig. 4.

Step 5

Position the gage/tape assembly so that the triangle alignment marks on the gage are over the layout lines on the specimen (Fig. 5). If the assembly appears to be misaligned, lift one end of the tape at a shallow angle until the assembly is free of the specimen. Realign properly, and firmly anchor down at least one end of the tape to the specimen. Realignment can be done without fear of contamination by the tape mastic if Micro-Measurements No. PCT-2A cellophane tape is used, because this tape will retain its mastic when removed.

Step 6

Lift the gage end of the tape assembly at a shallow angle to the specimen surface (about 45 degrees) until the gage and terminal are free of the specimen surface (Fig. 6a). Continue lifting the tape until it is free from the specimen approximately 1/2 in *(10 mm)* beyond the terminal. Tuck the loose end of the tape under and press to the specimen surface (Fig. 6b) so that the gage and terminal lie flat, with the bonding surface exposed.

Note: Micro-Measurements gages have been treated for optimum bonding conditions and require no pre-cleaning before use unless contaminated during handling. If contaminated, the back of any gage can be cleaned with a cotton-tipped applicator slightly moistened with M-Prep Neutralizer 5A.

Step 7

M-Bond 200 catalyst can now be applied to the bonding surface of the gage and terminal. M-Bond 200 adhesive will harden without the catalyst, but less quickly and reliably. Very little catalyst is needed and should be applied in a thin, uniform coat. Lift the brush-cap out of the catalyst bottle and wipe the brush approximately 10 strokes against the lip of the bottle to wring out most of the catalyst. Set the brush down on the gage and swab the gage backing (Fig. 7). Do not stroke the brush in a painting style, but slide the brush over the entire gage surface and then the terminal. Move the brush to the adjacent tape area prior to lifting from the surface. Allow the catalyst to dry at least one minute under normal ambient conditions of +75°F *(+24°C)* and 30% to 65% relative humidity before proceeding.

Note: The next three steps must be completed in the sequence shown, within 3 to 5 seconds. Read Steps 8, 9, and 10 before proceeding.

Step 8

Lift the tucked-under tape end of the assembly, and, holding in the same position, apply one or two drops of M-Bond 200 adhesive at the fold formed by the junction of the tape and specimen surface (Fig. 8). This adhesive application should be approximately 1/2 in *(13 mm)* outside the actual gage installation area. This will insure that local polymerization, taking place when the adhesive comes in contact with the specimen surface, will not cause uneveness in the gage glueline.

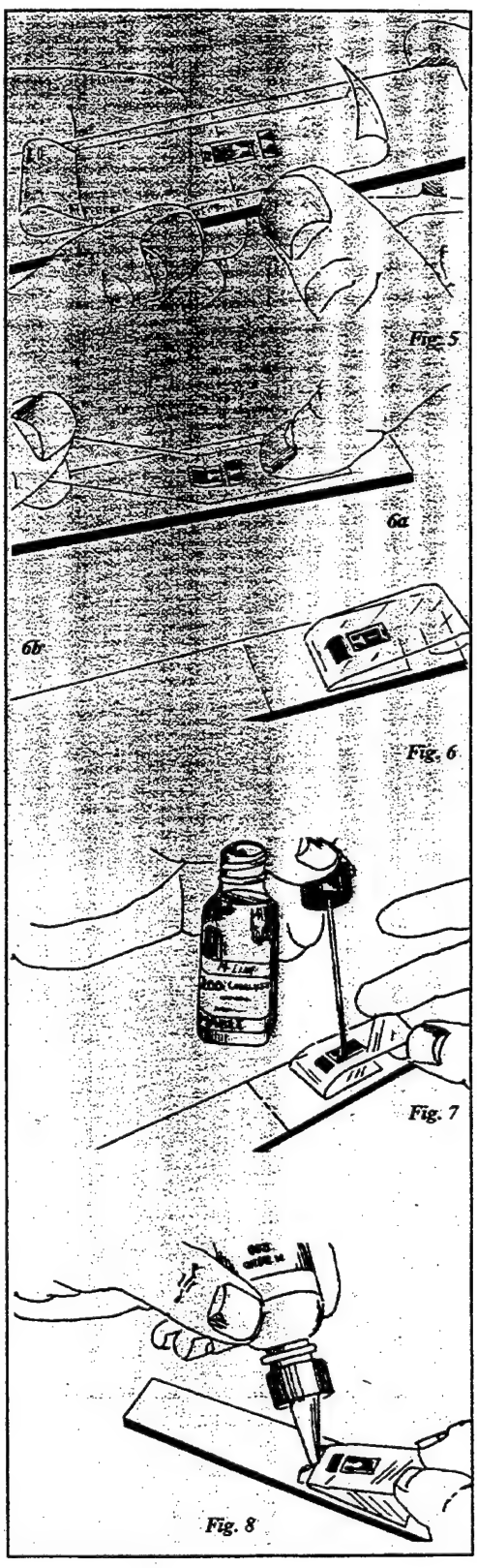

Fig. 5

Fig. 6

Fig. 7

Fig. 8

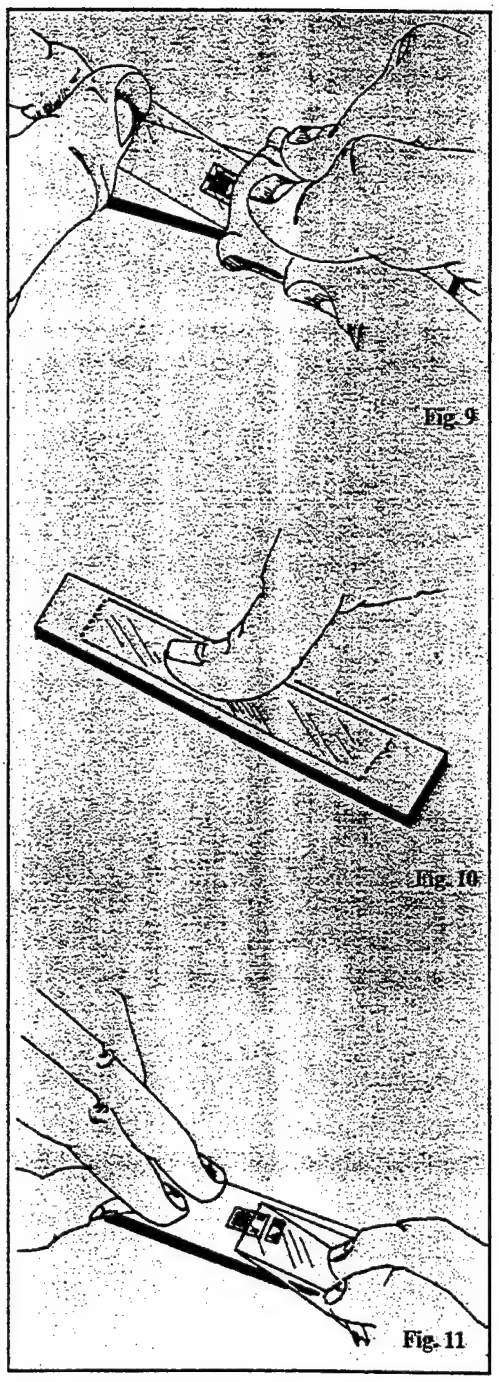

Fig. 9

Fig. 10

Fig. 11

Step 9

Immediately rotate the tape to approximately a 30-degree angle so that the gage is bridged over the installation area. While holding the tape slightly taut, slowly and *firmly* make a single wiping stroke over the gage/tape assembly with a piece of gauze (Fig. 9) bringing the gage back down over the alignment marks on the specimen. Use a firm pressure with your fingers when wiping over the gage. A very thin, uniform layer of adhesive is desired for optimum bond performance.

Step 10

Immediately upon completion of wipe-out of the adhesive, firm thumb pressure must be applied to the gage and terminal area (Fig. 10). This pressure should be held for at least one minute. In low humidity conditions (below 30%) or if the ambient temperature is below +70°F *(+20°C)*, this pressure application time may have to be extended to several minutes. Where large gages are involved, or where curved surfaces such as fillets are encountered, it may be advantageous to use preformed pressure padding during the operation. Pressure-application time should again be extended due to the lack of "thumb heat" which helps to speed adhesive polymerization. Wait two minutes before removing tape.

Step 11

The gage and terminal strip are now solidly bonded in place. To remove the tape, pull it back directly over itself, peeling it slowly and steadily off the surface (Fig. 11). This technique will prevent possible lifting of the foil on open-faced gages or other damage to the installation. It is not necessary to remove the tape immediately after gage installation. The tape will offer mechanical protection for the grid surface and may be left in place until it is removed for gage wiring.

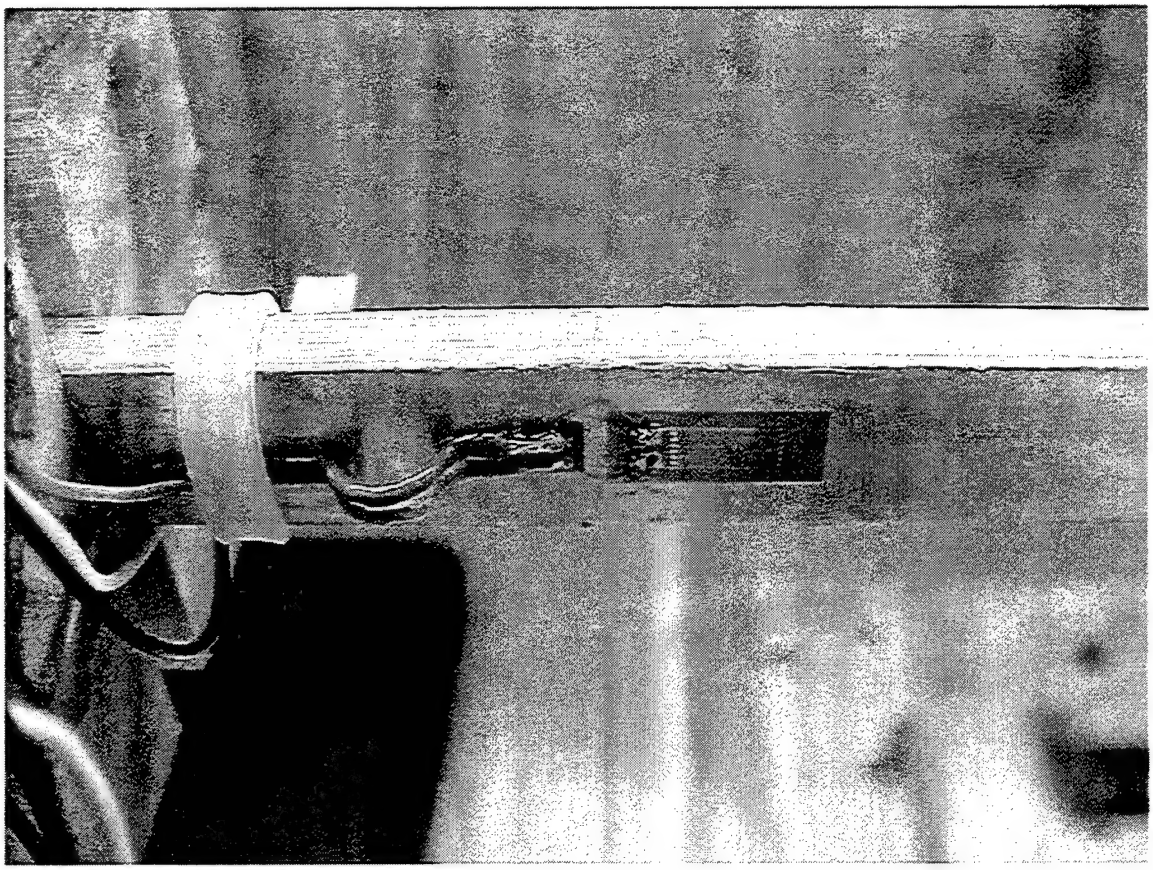

Figure 29. Photograph of the Fuel Beam Strain Gage

THIS PAGE IS INTENTIONALLY LEFT BLANK

APPENDIX F. AFTERBURNER FUEL SPRAY BARS

PURPOSE: Design the fuel spray bars for an afterburning section of a turbo-ramjet combined cycle engine (CCE).

DISCUSSION: Designing an afterburning section for the ramjet section of the CCE poses several problems. There must be adequate fuel delivery in low altitude flight regimes and metered flow at higher altitudes.

PROCEDURE: The spray bars for fuel delivery were set up in a concentric pattern similarly to most modern afterburning jet engines. Several different pressures were used, .1 MPa, .2 MPa, .3 MPa, and .4 MPa. The smallest possible holes for fuel delivery were used.

RESULTS: Low to high pressure settings were used. Spray pattern / pressure .1 MPa and .4 MPa / are shown in Figures (30), (31), (32) and (33). It was apparent that an addition spray ring would be required to properly atomize fuel. Once these rings were in place, a much finer fuel atomization was produced.

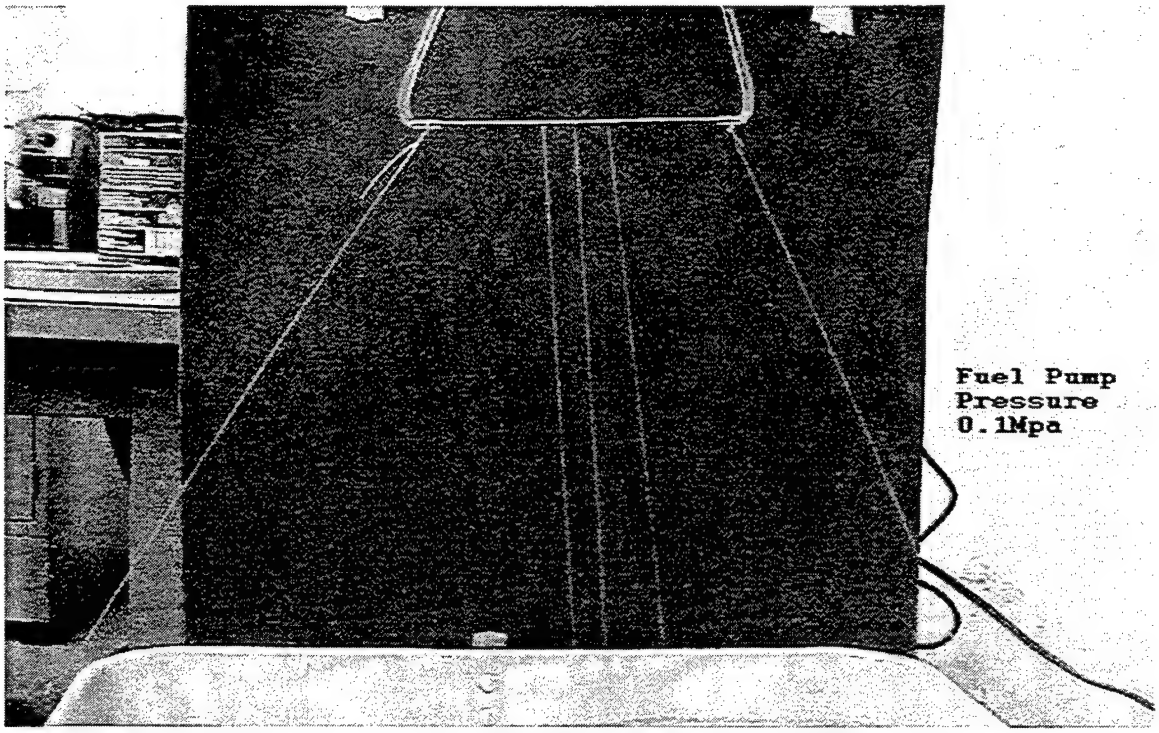

Figure 30. Photograph of the Fuel Spray Bar with no Diffusion Rings

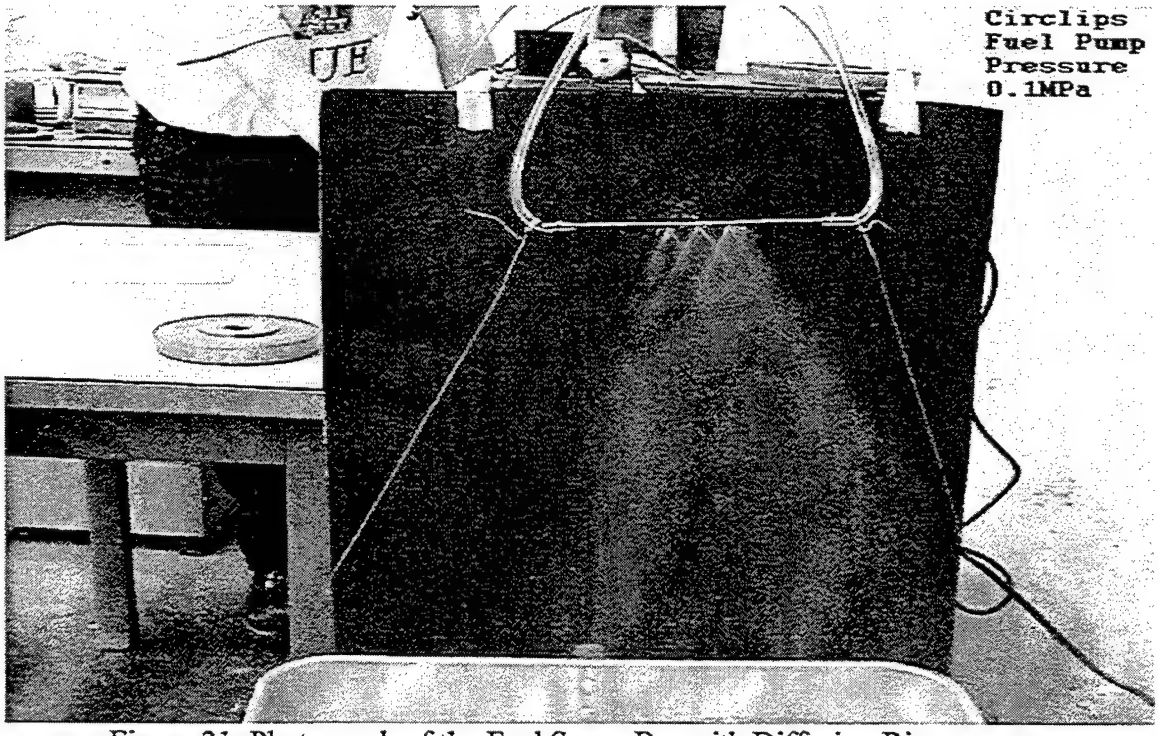

Figure 31. Photograph of the Fuel Spray Bar with Diffusion Rings

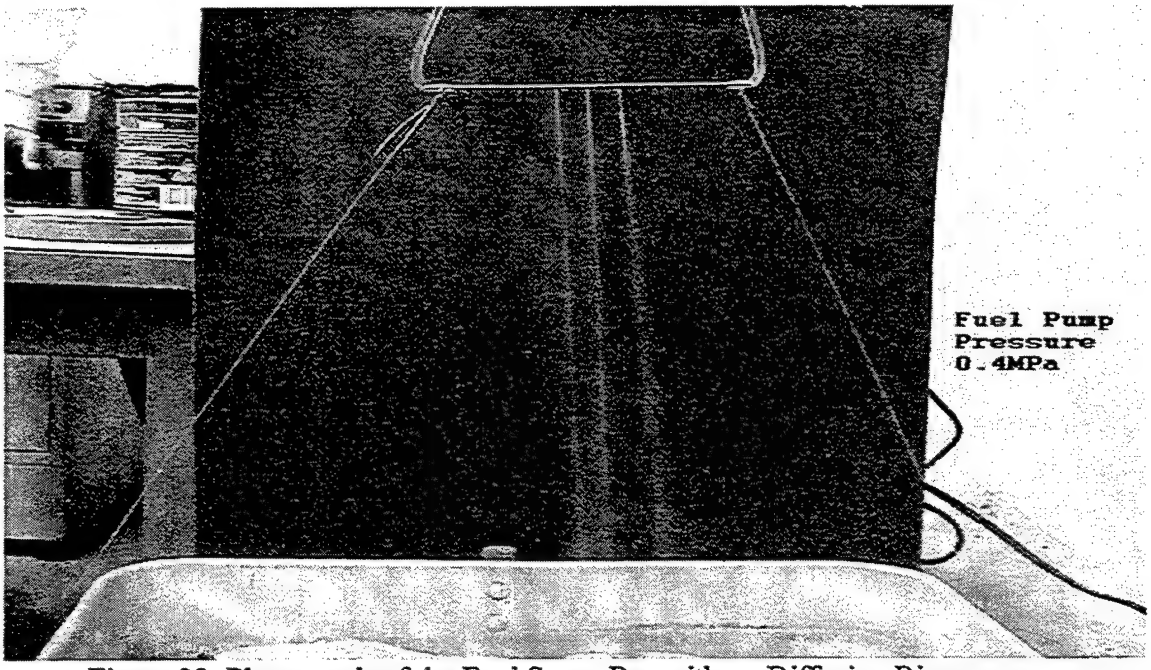

Figure 32. Photograph of the Fuel Spray Bar with no Diffusion Rings

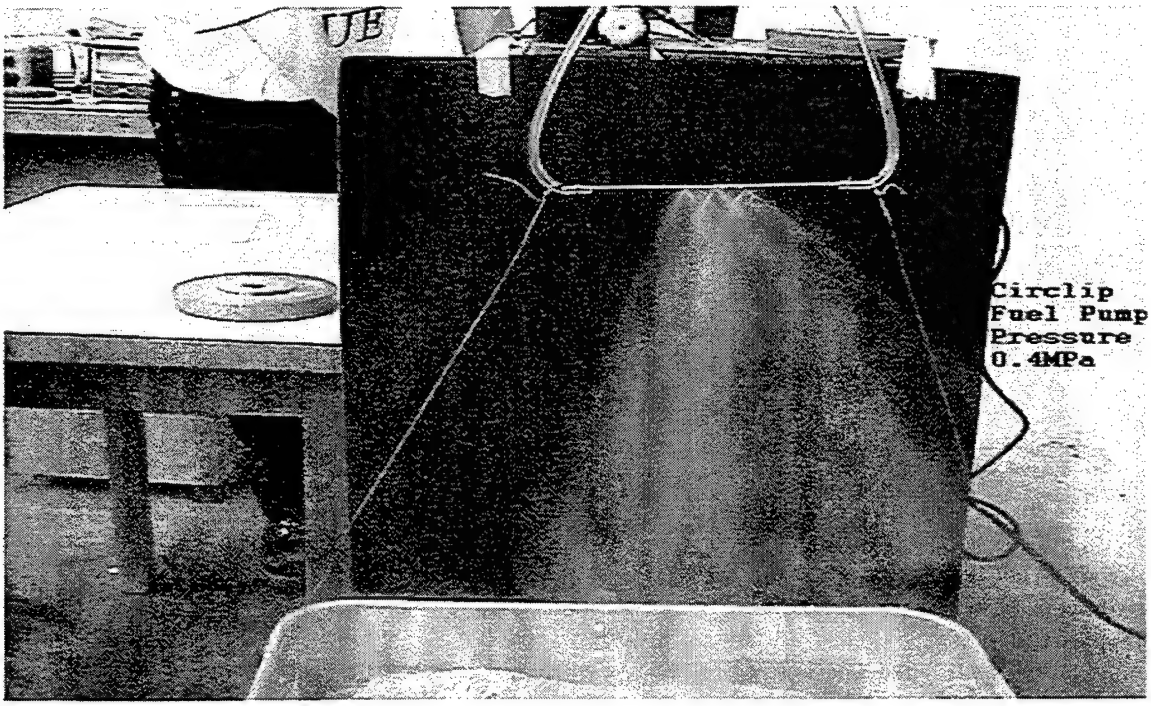

Figure 33. Photograph of the Fuel Spray Bar with Diffusion Rings

THIS PAGE IS INTENTIONALLY LEFT BLANK

APPENDIX G. OVERFLOW PROGRAM INPUT AND OUTPUT FILES

```
$GLOBAL
    CHIMRA= .F.,   NSTEPS=14000,   RESTRT= .F.,   NSAVE =10,
    NQT   = 202,
    $END
$FLOINP
    ALPHA =0.0,  FSMACH= 2.00,  REY   = 6.00E6,  TINF  = 520.000,
    $END
$VARGAM
    $END
$GRDNAM
    NAME = 'conic inlet 99,99,3',
$END
$NITERS
    $END
$METPRM
    IRHS  = 0,   ILHS  = 2,   IDISS  = 2,
    $END
$TIMACU
    DT    = .5, ITIME= 1,  TFOSO = 1.00, CFLMIN=0.01,
    $END
$SMOACU
    ISPECJ= 2,  DIS2J = 2.00,  DIS4J = 0.2,
    ISPECK= 2,  DIS2K = 2.00,  DIS4K = 0.2,
    ISPECL= 2,  DIS2L = 2.00,  DIS4L = 0.2,
    SMOO  = 1.00,
    EPSE  = 0.35,
    $END
$VISINP
    VISC = .T.,
    CFLT = 2,
    ITERT = 3,
    $END
$BCINP
    NBC   =  8,
    IBTYP =     5,  14,  32,  30,  33,   5,  5,   22,
    IBDIR =    -1,   2,   1,  -2,  -2,  -1,  1,   3,
    JBCS  =    -1,   1,   1,   1,  51,  50, 50,   1,
    JBCE  =    -1,  -1,   1,  50,  -1,  50, 50,  -1,
    KBCS  =     1,   1,   1,  -1,  -1,  50, 50,   1,
    KBCE  =    -1,   1,  -1,  -1,  -1,  -1, -1,  -1,
    LBCS  =     1,   1,   1,   1,   1,   1,  1,   1,
    LBCE  =    -1,  -1,  -1,  -1,  -1,  -1, -1,   1,
    BCPAR1(5)=3.3
    $END
$SCEINP
$END
```

```
        OVERFLOW  --  OVERLAPPED GRID FLOW SOLVER
            VERSION 1.8b   25 March 1998


 Compile time: Sun May 10 21:39:33 PDT 1998

 Current time: Mon Nov 13 09:22:59 2000




 GLOBAL PARAMETERS                              ($GLOBAL)
    CHIMERA STYLE INPUT?                         (CHIMRA) = F
    RUN INCORE?                                  (INCORE) = F
    RUNNING CDISC INVERSE DESIGN?                (CDISC ) = F
    NUMBER OF STEPS                              (NSTEPS) = 14000
    READ RESTART FILE?                           (RESTRT) = F
    SAVE RESTART FILE EVERY                      (NSAVE )       10 STEPS
    COMPUTE FORCE/MOMENT COEFS EVERY             (NFOMO )       10 STEPS
    TURBULENCE MODEL TYPE                        (NQT)     =   202
    NUMBER OF SPECIES                            (NQC)     =     0
    USE MULTIGRID?                               (MULTIG) = F
    USE FULL MULTIGRID?                          (FMG)    = F
    NO. OF GRID LEVELS (IF MULTIG=.T.)           (NGLVL)   =     3
    NO. OF FMG CYCLES (IF FMG=.T.)               (FMGCYC)  =     0     0
    MAX NUMBER OF NEWTON SUBITERATIONS           (NITNWT)  =     0
    NO. ORDERS CONVERGENCE FOR NEWTON SUB        (ORDNWT)  =      0.00000
    FIRST/SECOND ORDER NEWTON SUB (0-2)          (FSONWT)  =      2.00000

 ALLOCATING MEMORY FOR GRID AND FLOWFIELD ARRAYS:

    REQUESTING      470448 REAL    WORDS FOR FLOWFIELD ARRAYS (Q,S)
    REQUESTING      470448 REAL    WORDS FOR GRID ARRAYS (X,Y,Z,METRICS)
    REQUESTING       29403 INTEGER WORDS FOR GRID ARRAY  (IBLANK)
    REQUESTING      324423 REAL    WORDS FOR TEMPORARY ARRAYS (TMP,TMP2,TMP3)

 ** NOTE ** Turning off force/moment reporting since input files
            (mixsur.fmp, grid.ibi and grid.ptv) do not exist.

 FLOW CONDITIONS                                 ($FLOINP)
    ANGLE OF ATTACK (DEG)                       (ALPHA ) =    0.00000
    SIDESLIP        (DEG)                       (BETA  ) =    0.00000
    FREESTREAM MACH NUMBER                      (FSMACH) =    2.00000
    SPECIFIC HEAT RATIO                         (GAMINF) =    1.40000
    REYNOLDS NUMBER                             (REY   ) =  0.60000E+07
    PRANDTL NUMBER                              (PR    ) =    0.72000
    TURBULENT PRANDTL NUMBER                    (PRT   ) =    0.90000
    FREESTREAM TEMP (DEG R)                     (TINF  ) =  520.00000
    FREESTREAM KINETIC ENERGY (K/VINF^2)        (XKINF ) =  0.10000E-03
    FREESTREAM TURB LEVEL (MU_T/MU_L)           (RETINF) =    0.10000

 VARIABLE GAMMA / MULTIPLE SPECIES               ($VARGAM)
    GAMMA CALCULATION METHOD (0-2)              (IGAM  ) =     0
    TOTAL ENTHALPY RATIO FOR ALL GAS 1          (HT1   ) =   10.00000
    TOTAL ENTHALPY RATIO FOR ALL GAS 2          (HT2   ) =   10.00000


 INPUTS FOR GRID     1:

    GRID NAME                                    ($GRDNAM)
         conic inlet 99,99,3                        (NAME  )

    NUMBER OF TIME STEPS./ ITERATIONS            ($NITERS)
         ITERATIONS PER STEP                        (ITER  ) =     1
```

```
METHOD CONTROL PARAMETERS                    ($METPRM)
     RIGHT-HAND-SIDE OPTION FLAG               (IRHS  ) =      0
     LEFT-HAND-SIDE OPTION FLAG                (ILHS  ) =      2
     DISSIPATION OPTION FLAG                   (IDISS ) =      2
     LOW-MACH PRECONDITIONING PARAMETER        (BIMIN ) =       1.00000
     LOCAL MULTIGRID OPTION                    (MULTIG) = F
     PROLONGATION SMOOTHING PARAMETERS         (SMOOPJ) =       0.00000
           (IF MULTIG=.T.)                     (SMOOPK) =       0.00000
                                               (SMOOPL) =       0.00000
     CORRECTION SMOOTHING PARAMETERS           (SMOOCJ) =       0.00000
           (IF MULTIG=.T.)                     (SMOOCK) =       0.00000
                                               (SMOOCL) =       0.00000
     RESIDUAL SMOOTHING PARAMETERS             (SMOORJ) =       0.00000
           (IF MULTIG=.T.)                     (SMOORK) =       0.00000
                                               (SMOORL) =       0.00000
     USE VISCOUS TERMS ON COARSE LEVELS?       (CORSVI) = F
     RECOMPUTE MU_T ON FINEST LEVEL?           (RECMUT) = F

TIME STEP/ACCURACY PARAMETERS                ($TIMACU)
     TIME STEP SCALING OPTION FLAG (0-2)       (ITIME ) =      1
     RELAXATION FACTOR OPTION FLAG (0-1)       (IRELAX) =      0
     TIME STEP                                 (DT    ) =       0.50000
     FIRST/SECOND ORDER IN TIME (1-2)          (TFOSO ) =       1.00000
     MINIMUM CFL NUMBER                        (CFLMIN) =       0.01000
     MAXIMUM CFL NUMBER                        (CFLMAX) =       0.00000

SPATIAL SMOOTHING/ACCURACY PARAMETERS ($SMOACU)
     SPECTRAL RAD SMOOTHING (-1,1,2,3)         (ISPECJ) =      2
                                               (ISPECK) =      2
                                               (ISPECL) =      2
     SPECTRAL RAD VS VEL SMOOTHING (0-1)       (SMOO  ) =       1.00000
     2ND O SMOOTHING COEFS (ARC3D-TYPE)        (DIS2J ) =       2.00000
                                               (DIS2K ) =       2.00000
                                               (DIS2L ) =       2.00000
     4TH O SMOOTHING COEFS (ARC3D-TYPE)        (DIS4J ) =       0.20000
                                               (DIS4K ) =       0.20000
                                               (DIS4L ) =       0.20000
     CENTRAL DIFF SMOOTHING (F3D-TYPE)         (EPSE  ) =       0.35000
     LU-SGS SPECTRAL RADIUS EPSILON            (EPSSGS) =       0.02000
     ROE LIMITER FIX PARAMETER                 (DELTA ) =       1.00000
     FLUX-SPLIT 1ST/2ND/3RD ORDER (1-3)        (FSO   ) =       2.00000
     MATRIX DISSIPATION LINEAR LIMIT           (VEPSL ) =       0.00000
     MATRIX DISSIPATION NONLIN. LIMIT          (VEPSN ) =       0.00000
     USE ROE AVERAGE IN MATRIX DISSIP?         (ROEAVG) = F

VISCOUS/INVISCID FLAGS                       ($VISINP)
     INCLUDE VISCOUS TERMS IN  J?              (VISCJ ) = T
                               K?              (VISCK ) = T
                               L?              (VISCL ) = T
     INCLUDE VISCOUS CROSS TERMS?              (VISCX ) = T

TURBULENT SURFACE SPECS                      ($VISINP)
     NUMBER OF TURBULENT SURFACE SPECS         (NTURB ) =  -999

TURBULENCE MODEL PARAMETERS                  ($VISINP)
     ITERATIONS PER FLOW SOLVER ITERATION      (ITERT ) =      3
     LOCAL TIME STEP CONSTANT                  (CFLT  ) =       2.00000
     UPWIND DIFFERENCING FLAG (0-1)            (IUPT  ) =      1
     2ND O SMOOTHING COEF (ARC3D-TYPE)         (DIS2T ) =       2.00000
     4TH O SMOOTHING COEF (ARC3D-TYPE)         (DIS4T ) =       0.04000

BOUNDARY CONDITION SPECS                     ($BCINP )
     NUMBER OF BOUNDARY CONDITION SPECS        (NBC   ) =      8
       (IBTYP) (IBDIR) (JBCS) (JBCE) (KBCS) (KBCE) (LBCS) (LBCE)
            5      -1     -1     -1      1     -1      1     -1
```

```
              14       2       1      -1       1       1       1      -1
              32       1       1       1       1      -1       1      -1
              30      -2       1      50      -1      -1       1      -1
              33      -2      51      -1      -1      -1       1      -1
               5      -1      50      50      50      -1       1      -1
               5       1      50      50      50      -1       1      -1
              22       3       1      -1       1      -1       1       1

   SPECIES CONTINUITY EQN PARAMETERS      ($SCEINP)
        ITERATIONS PER FLOW SOLVER ITERATION(ITERC ) =      1
        LOCAL TIME STEP CONSTANT             (CFLC  ) =      1.00000
        UPWIND DIFFERENCING FLAG (0-1)       (IUPC  ) =     0
        2ND O SMOOTHING COEF (ARC3D-TYPE)    (DIS2C ) =      2.00000
        4TH O SMOOTHING COEF (ARC3D-TYPE)    (DIS4C ) =      0.04000

GRID SIZE FOR GRID     1:

   NUMBER OF POINTS IN J  (JD    ) =    99
                       K  (KD    ) =    99
                       L  (LD    ) =     3

CHECKING BOUNDARY CONDITIONS FOR GRID     1:

     1)  BOUNDARY CONDITION TYPE#      5     DIRECTION    -1
      VISCOUS ADIABATIC SOLID WALL  (PRESSURE EXTRAPOLATION)
        SLOW-START FROM FREE STREAM WILL BE USED
      DIR=-1    J-RANGE=   99   99    K-RANGE=    1   99    L-RANGE=    1    3
     2)  BOUNDARY CONDITION TYPE#     14     DIRECTION     2
      AXIS IN K (J AROUND)
       1.00 ORDER EXTRAPOLATION FOR ZERO SLOPE
      DIR= 2    J-RANGE=    1   99    K-RANGE=    1    1    L-RANGE=    1    3
     3)  BOUNDARY CONDITION TYPE#     32     DIRECTION     1
      SUPERSONIC/SUBSONIC INFLOW/OUTFLOW
      DIR= 1    J-RANGE=    1    1    K-RANGE=    1   99    L-RANGE=    1    3
     4)  BOUNDARY CONDITION TYPE#     30     DIRECTION    -2
      OUTFLOW (EXTRAPOLATION)
      DIR=-2    J-RANGE=    1   50    K-RANGE=   99   99    L-RANGE=    1    3
     5)  BOUNDARY CONDITION TYPE#     33     DIRECTION    -2
      SPECIFIED PRESSURE OUTFLOW
        P/PINF =    3.30000
        SLOW-START FROM FREE STREAM WILL BE USED
      DIR=-2    J-RANGE=   51   99    K-RANGE=   99   99    L-RANGE=    1    3
     6)  BOUNDARY CONDITION TYPE#      5     DIRECTION    -1
      VISCOUS ADIABATIC SOLID WALL  (PRESSURE EXTRAPOLATION)
        SLOW-START FROM FREE STREAM WILL BE USED
        NOTE   : CONDITION NOT SPECIFIED AT PLANE 1 OR LAST
      DIR=-1    J-RANGE=   50   50    K-RANGE=   50   99    L-RANGE=    1    3
     7)  BOUNDARY CONDITION TYPE#      5     DIRECTION     1
      VISCOUS ADIABATIC SOLID WALL  (PRESSURE EXTRAPOLATION)
        SLOW-START FROM FREE STREAM WILL BE USED
        NOTE   : CONDITION NOT SPECIFIED AT PLANE 1 OR LAST
      DIR= 1    J-RANGE=   50   50    K-RANGE=   50   99    L-RANGE=    1    3
     8)  BOUNDARY CONDITION TYPE#     22     DIRECTION     3
      AXISYMMETRIC CONDITION IN Y, IN L (ROTATE -1/0/+1 DEGREE ABOUT X AXIS)
      DIR= 3    J-RANGE=    1   99    K-RANGE=    1   99    L-RANGE=    1    1

CHECKING VISCOUS AND TURBULENCE MODELING SPECIFICATIONS FOR GRID     1:

   K-OMEGA 2-EQUATION TURBULENCE MODEL SELECTED


** WARNING ** (VISCL) L-DIRECTION VISCOUS TERMS TURNED OFF BECAUSE
                  GRID IS AXISYMMETRIC IN L.

   INCLUDE VISCOUS TERMS IN J-DIRECTION
   INCLUDE VISCOUS TERMS IN K-DIRECTION
```

APPENDIX H. GRIDGEN INPUT PARAMETERS

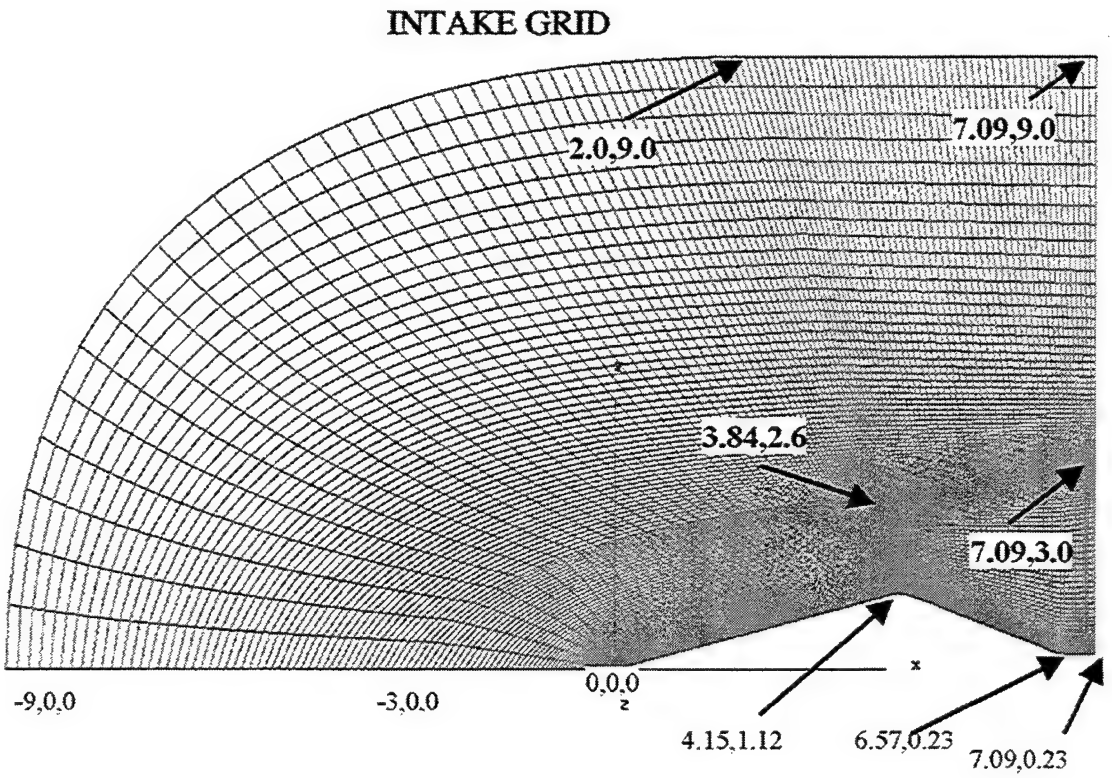

Figure 34. Grid Parameters

THIS PAGE IS INTENTIONALLY LEFT BLANK

LIST OF REFERENCES

1. Rivera, G., *Turbochargers to Small Turbojet Engine for Uninhabited Aerial Vehicles*, Engineer's Thesis, Department of Aeronautics and Astronautics, U.S. Naval Postgraduate School, Monterey, CA, June 1998

2. Lobik, L.P. *Unmanned Aerial Vehicles: A Study of Gas Turbine Application*, Master's Thesis, Department of Aeronautics and Astronautics, U.S. Naval Postgraduate School, Monterey, CA, September 1995

3. Kurzke, J., *GASTURB 7.0 for Windows A Program to Calculate Design and Off Design Performance Of Gas Turbines, 1996*

4. Hackaday, G. L. *Thrust Augmentation For a Small Turbojet Engine,* Master's Thesis, Department of Aeronautics and Astronautics, U.S. Naval Postgraduate School, Monterey, CA, June 1998

5. Andreou, L. *Performance of a Ducted Micro Turbojet Engine,* Master Thesis Department of Aeronautics and Astronautics, U.S. Naval Postgraduate School, Monterey, CA, September 1999

6. Al-Namani S. M. *Development of Shrouded Turbojet to Form a Turboramjet for Future Missile Applications*, Master Thesis Department of Physics, U.S. Naval Postgraduate School, Montery, CA, June 2000

7. Buning,P.G., Chiu, I.J., Obaya, S., Rizk, Y.M., and Steger, I.L., *Numerical Simulation of the Integrated Space Shuttle Vehicle in Ascent*, AIAA Atmospheric Flight Mechanics Conference, Minneapolis, Minnesota, August, 1998

8. Fan, Y.S., *An Investigation of the Transonic Viscous Drag Coefficient for Axisymetric Bodies*, Master of Science in Aeronautical Engineering, Naval Postgraduate School, March, 1995

9. Steinbrenner, J.P., and Chawner, J.R., *GRIDGEN Release Notes Version 9.6*, MDA Engineering, Arlington Texas, October, 1994

THIS PAGE IS INTENTIONALLY LEFT BLANK

INITIAL DISTRIBUTION LIST

1 Defense Technical Information Center.....2
8725 John J. Kingman Rd., Suite 0944
Ft Belvoir, VA 22060-6218

2 Dudley Knox Library.....2
Naval Postgraduate School
411 Dyer Rd
Monterey, CA 93943-5101

3 Prof William B. Maier.....1
Chairman, Department of Physics
Naval Postgraduate School
699 Dyer Road, Room 203
Monterey, CA 93943-5106

4 Prof Garth V Hobson, Code Aa/Hg.....5
Department of Aeronautics and Astronautics
Naval Postgraduate School
699 Dyer Road, Room 137
Monterey, CA 93943-5106

5 Prof K.E.Woehler, Code Ph/Wh.....1
Department of Physics
Naval Postgraduate School
699 Dyer Road, Room 206B
Monterey, CA 93943-5106

6 Naval Air Warfare Center Aircraft Division.....1
Propulsion and Power Engineering
22195 Elmer Road
Patuxent River, MD 20670-5305
ATTN: J Carroll, Code 4.4.3.2, BLDG 1461

7 Naval Air Warfare Center Aircraft Division.....1
Propulsion and Power Engineering
22195 Elmer Road
Patuxent River, MD 20670-5305
ATTN: C. Georgio, Code 4.4

8 LCDR Hector Garcia.....2
29085 Greenspot Road
Highland, CA 92346